Received 13 February 2017; | Revised **3 July 2018 (revised preprint with corrections)** ; | Accepted 22 August 2017

DOI: 10.1002/mma.4597 is revision 18 Sep 2017, published in *Mathematical Methods in the Applied Sciences*, 41(11)4088–4105, 30 July 2018, Special Issue: ENGAGE

SPECIAL ISSUE PAPER

Triple Conformal Geometric Algebra for Cubic Plane Curves

Robert Benjamin Easter[1] | Eckhard Hitzer[2]

[1]Bangkok, Thailand. Email: reaster2015@gmail.com

[2]College of Liberal Arts, International Christian University, 3-10-2 Osawa, 181-8585 Mitaka, Tokyo, Japan. Email: hitzer@icu.ac.jp

Communicated by: Dietmar Hildenbrand

MSC Primary: 15A66;

MSC Secondary: 14H50; 53A30;

Correspondence

Eckhard Hitzer, College of Liberal Arts, International Christian University, 3-10-2 Osawa, 181-8585 Mitaka, Tokyo, Japan. Email: hitzer@icu.ac.jp

Summary

The Triple Conformal Geometric Algebra (TCGA) for the Euclidean $\mathbb{R}^2$-plane extends CGA as the product of three orthogonal CGAs, and thereby the representation of geometric entities to general cubic plane curves and certain cyclidic (or roulette) quartic, quintic, and sextic plane curves. The plane curve entities are 3-vectors that linearize the representation of non-linear curves, and the entities are inner product null spaces (IPNS) with respect to all points on the represented curves. Each IPNS entity also has a dual geometric outer product null space (OPNS) form. Orthogonal or conformal (angle-preserving) operations (as versors) are valid on all TCGA entities for inversions in circles, reflections in lines, and, by compositions thereof, isotropic dilations from a given center point, translations, and rotations around arbitrary points in the plane. A further dimensional extension of TCGA, also provides a method for anisotropic dilations. Intersections of any TCGA entity with a point, point pair, line or circle are possible. TCGA defines commutator-based differential operators in the coordinate directions that can be combined to yield a general **n**-directional derivative.

KEYWORDS:

Clifford algebra, cubic plane curve, conformal geometric algebra, 3-vector entity

1 | INTRODUCTION

This paper[1] assumes familiarity with Clifford's geometric algebras (GA) $\mathcal{G}_{p,q}$ [14] over an $(n = p + q)$-dimensional (n-D) pseudo-Euclidean[2] vector space $\mathbb{R}^{p,q}$ over real numbers $\mathbb{R}$, and with the general theory of the corresponding Conformal Geometric Algebra (CGA) [23] $\mathcal{G}_{p+1,q+1}$, especially for an $(n = p)$-D Euclidean vector space $\mathbb{R}^n$. References [3] and [25] are books that include full discussions of CGA $\mathcal{G}_{4,1}$ for modeling three-dimensional Euclidean space $\mathbb{R}^3$. The paper [19] shows different aspects of $\mathcal{G}_{4,1}$, its quaternionic subalgebra structure, its relationship with Minkowski space algebra, and a self-contained Java implementation. Moreover, [21] provides a short self-contained general purpose tutorial for Clifford's geometric algebra (including CGA). See also [20], with an emphasis on common geometric features of the basic flat and round entities in CGA.

As further background, it is also helpful to have familiarity with the recently introduced *Double Conformal Geometric Algebra* (DCGA) $\mathcal{G}_{2(3+1),2(0+1)} = \mathcal{G}_{8,2}$ [5] for $\mathbb{R}^3$, and with the *Double Conformal Space-Time Algebra* (DCSTA) $\mathcal{G}_{2(1+1),2(3+1)} = \mathcal{G}_{4,8}$ for the Minkowski pseudo-Euclidean vector space $\mathbb{R}^{1,3}$ [9][6].

The CGA $\mathcal{G}_{p+1,q+1}$ non-linearly embeds the vector space $\mathbb{R}^{p,q}$ for which geometric entities are modeled conformally.

[1]This revised version (3 July 2018) includes corrections to the published version (18 Sep 2017), which is published as DOI:10.1002/mma.4597 in the journal *Mathematical Methods in the Applied Sciences*, 41(11):4088–4105, 30 July 2018, Special Issue: Empowering Novel Geometric Algebra in Graphics and Engineering (ENGAGE). The special issue contains full/long papers from the Computer Graphics International 2017 (CGI'17), **Empowering Novel Geometric Algebra for Graphics and Engineering (ENGAGE) Workshop** held Tuesday 27th June 2017 in Yokohama, Japan. We thank the ENGAGE Workshop organizers: Andreas Aristidou (a.m.aristidou@gmail.com), Dietmar Hildenbrand (dietmar.hildenbrand@gmail.com), Eckhard Hitzer (hitzer@icu.ac.jp), G. Stacey Staples (sstaple@siue.edu), Werner Benger, Olav Egeland, George Papagiannakis, Kanta Tachibana, and Yu Zhaoyuan.

[2]We use *Euclidean* for vector spaces with $n = p$, $q = 0$, and *pseudo-Euclidean* for vector spaces with $p < n$, $q > 0$.

The use of CGA can be motivated[3] by a consideration of *stereographic embedding*: In [25], the conformal embedding $C(\mathbf{t})$ is defined as a *stereographic embedding* followed by a Minkowski *homogenization*. The stereographic embedding of $\mathbf{t} \in \mathbb{R}^2$, denoted $S(\mathbf{t})$, is the point on the unit 2-sphere centered on the origin in $\mathbb{R}^3(\mathbf{e}_1, \mathbf{e}_2, \mathbf{e}_+)$ where the line $\mathbf{e}_+ + t\hat{\mathbf{d}}$, with $\mathbf{d} = \mathbf{t} - \mathbf{e}_+$, intersects the unit circle around the origin in the $\hat{\mathbf{t}}\mathbf{e}_+$-plane. $S(\mathbf{t})$ can be solved by similar triangles as

$$S(\mathbf{t}) = \frac{2\|\mathbf{t}\|}{\|\mathbf{t}\|^2 + 1}\hat{\mathbf{t}} + \frac{\|\mathbf{t}\|^2 - 1}{\|\mathbf{t}\|^2 + 1}\mathbf{e}_+. \tag{1}$$

The Minkowski *homogenization* is $\mathcal{H}_{\mathcal{M}}(\mathbf{t}) = S(\mathbf{t}) + \mathbf{e}_- \in \mathbb{R}^{3,1}$. Since $\mathcal{H}_{\mathcal{M}}(\mathbf{t})$ is homogeneous, it can be scaled by an arbitrary non-zero scalar without affecting the point that is represented. The common practice is to define the final conformal embedding as

$$\begin{aligned} C(\mathbf{t}) &= \frac{\|\mathbf{t}\|^2 + 1}{2}\left(S(\mathbf{t}) + \mathbf{e}_-\right) && (2)\\ &= \frac{\|\mathbf{t}\|^2 + 1}{2}\left(\frac{2\|\mathbf{t}\|}{\|\mathbf{t}\|^2 + 1}\hat{\mathbf{t}} + \frac{\|\mathbf{t}\|^2 - 1}{\|\mathbf{t}\|^2 + 1}\mathbf{e}_+ + \mathbf{e}_-\right) && (3)\\ &= \mathbf{t} + \frac{\mathbf{t}^2}{2}\left(\mathbf{e}_- + \mathbf{e}_+\right) + \frac{1}{2}\left(\mathbf{e}_- - \mathbf{e}_+\right) && (4)\\ &= \mathbf{t} + \frac{\mathbf{t}^2}{2}\mathbf{e}_{\infty 1} + \mathbf{e}_{o1}. && (5) \end{aligned}$$

For $\|\mathbf{t}\| = 0$, then $C(\mathbf{t}) \to \mathbf{e}_{o1}$, where

$$\mathbf{e}_{o1} = \frac{1}{2}\left(\mathbf{e}_- - \mathbf{e}_+\right) \tag{6}$$

is the entity for the *point at the origin*. In the limit as $\|\mathbf{t}\| \to \infty$, then $2C(\mathbf{t})/\|\mathbf{t}\|^2 \to \mathbf{e}_{\infty 1}$, where

$$\mathbf{e}_{\infty 1} = \mathbf{e}_- + \mathbf{e}_+ \tag{7}$$

is the entity for the *point at infinity*. In CGA2 and CGA3, the corresponding points are named $\{\mathbf{e}_{\infty 2}, \mathbf{e}_{o2}\}$ and $\{\mathbf{e}_{\infty 3}, \mathbf{e}_{o3}\}$, respectively. Since $S(\mathbf{t})$ is on the unit circle, then $\|S(\mathbf{t})\| = 1$ and $\left(S(\mathbf{t}) + \mathbf{e}_-\right)^2 = 0$ such that $C(\mathbf{t})$ is a *null vector*.

The CGA $\mathcal{G}_{p+1,q+1}$ can also be extended by multiplicity k to a k-CGA $\mathcal{G}_{k(p+1),k(q+1)}$ by multiplying k orthogonal copies of CGA, each with the same scalar coefficients on corresponding CGA basis blades. The main motivation for this approach is, that in k-CGA one can formulate k-vectors by linear combination of k-vector extraction operators for coordinate polynomials of degree k and (selectively) up to degree $2k$. These k-vectors represent algebraic curves of degree k to $2k$, which is generally not possible in standard CGA. The advantages of this formulation are the complete freedom to use linear versor operators for translation, rotation, dilation, reflection, inversion and transversion, and the freedom of intersection with standard CGA entities is preserved.

The paper is organized as follows. Section 2 introduces the (simple) CGA model for the Euclidean plane $\mathbb{R}^2$, and provides some motivation for the non-linear embedding of points in CGA. Next, Section 3 describes a triple version of the CGA model for the Euclidean plane $\mathbb{R}^2$, called TCGA. It describes how plane curves of degree three to six can be encoded as 3-vectors, how these curves can be transformed, intersected with simple CGA entities, and differentiated. It also includes selected examples of these curves, their TCGA expressions and graphs. Finally, Section 4 explains several aspects of computer algebra implementation of triple CGA. We conclude with Section 5. Appendix A explains computational details of efficient versor operations.

2 | CGA $\mathcal{G}_{2+1,1}$ OF THE EUCLIDEAN PLANE $\mathbb{R}^2$

The CGA $\mathcal{G}_{p+1,q+1}$ non-linearly embeds the $(n = p + q)$-dimensional vector space $\mathbb{R}^{p,q}$ for which geometric entities are modeled conformally[4]. These geometric entities in CGA represent points, point pairs, circles, spheres, hyperplanes, hyper(pseudo)spheres, and their intersections (by wedge products) in $\mathbb{R}^{p,q}$ (see [18]).

The *Conformal Geometric Algebra* (CGA) $\mathcal{G}_{3,1}$ of the Euclidean plane $\mathbb{R}^2$, also called the Compass Ruler Algebra [16], provides entities for points, lines, circles, and their intersections. The basis of $\mathbb{R}^{3,1}$ is given by four orthonormal vectors

[3] For the notation used in this paragraph, please refer to Section 2.

[4] In the framework of k-CGA, standard (single) CGA could be labeled 1-CGA. To avoid cluttered notation we omit this. The current section briefly reviews standard CGA of the Euclidean plane.

$\{\mathbf{e}_1, \mathbf{e}_2, \mathbf{e}_3 = \mathbf{e}_+, \mathbf{e}_4 = \mathbf{e}_-\}$, where the first three square to $+1$, and the last to -1. The unit pseudoscalar of the Euclidean plane $\mathbb{R}^2$ is $\mathbf{I}_\mathcal{E} = \mathbf{e}_1\mathbf{e}_2$. The unit pseudoscalar of $\mathcal{G}_{3,1}$ is $\mathbf{I}_C = \mathbf{e}_1\mathbf{e}_2\mathbf{e}_+\mathbf{e}_-$.

Notation 1. The symbolic test vector in the Euclidean plane is denoted by $\mathbf{t} = \mathbf{t}_\mathcal{E} = x\mathbf{e}_1 + y\mathbf{e}_2$, and a specific point by $\mathbf{p} = \mathbf{p}_\mathcal{E} = p_x\mathbf{e}_1 + p_y\mathbf{e}_2$.

Notation 2. The *reverse* $A^\sim$ of a multivector A reverses the order of all vector products in A (e.g., $\mathbf{I}_\mathcal{E}^\sim = \mathbf{e}_2\mathbf{e}_1$; in this case, $\mathbf{I}_\mathcal{E}^\sim = \mathbf{I}_\mathcal{E}^{-1} = -\mathbf{I}_\mathcal{E}$).

In the following subsections, we will introduce relevant multivector entities in CGA for geometric objects and for transformation operators.

2.1 | 2-D CGA null point entity

The CGA null *point* entity $\mathbf{T}_C = C(\mathbf{t})$ is the *conformal embedding*

$$C(\mathbf{t}) = \mathbf{t} + \frac{\mathbf{t}^2}{2}\mathbf{e}_{\infty 1} + \mathbf{e}_{o1} \tag{8}$$

of the $\mathcal{G}_2^1$ Euclidean vector[5] $\mathbf{t} \in \mathbb{R}^2$. The Minkowskian pair of null vectors representing origin and infinity is given by[6]

$$\mathbf{e}_o = \mathbf{e}_{o1} = \frac{1}{2}\left(\mathbf{e}_- - \mathbf{e}_+\right), \qquad \mathbf{e}_\infty = \mathbf{e}_{\infty 1} = \mathbf{e}_- + \mathbf{e}_+. \tag{9}$$

This implies that a conformally embedded point $C(\mathbf{t})$ squares itself to zero, $C(\mathbf{t})^2 = 0$ (i.e., it is also a null-vector). Furthermore, every finite conformal point is embedded, such that it is on the 3-D hyperplane in $\mathbb{R}^{3,1}$ defined by

$$C(\mathbf{t}) \cdot \mathbf{e}_{\infty 1} = -1, \tag{10}$$

which includes the origin point as well, since by construction $\mathbf{e}_{o1} \cdot \mathbf{e}_{\infty 1} = -1$.

A point $\mathbf{P}_C$ can be transformed to the normalized point $\hat{\mathbf{P}}_C$ that has unit scale on the homogeneous component $\mathbf{e}_{o1}$ as

$$\hat{\mathbf{P}}_C = \frac{\mathbf{P}_C}{-\mathbf{P}_C \cdot \mathbf{e}_{\infty 1}}. \tag{11}$$

Points are assumed to be initially normalized as the embedding $\hat{\mathbf{P}}_C = C\left(\mathbf{p}_\mathcal{E}\right)$. After performing operations on a point (or other entity), it may no longer be normalized. Some operations do not preserve the homogeneous scale.

The *projection* (inverse embedding) of a CGA *point* $\mathbf{P}_C$ back to a vector $\mathbf{p}_\mathcal{E} \in \mathbb{R}^2$ is

$$\mathbf{p}_\mathcal{E} = \left(\hat{\mathbf{P}}_C \cdot \mathbf{I}_\mathcal{E}\right)\mathbf{I}_\mathcal{E}^{-1}. \tag{12}$$

The Euclidean distance $d(\mathbf{p}, \mathbf{q})$ between two *finite* CGA points $\mathbf{P}_C = C(\mathbf{p})$ and $\mathbf{Q}_C = C(\mathbf{q})$ is

$$d\left(\mathbf{P}_C, \mathbf{Q}_C\right) = \sqrt{-2\hat{\mathbf{P}}_C \cdot \hat{\mathbf{Q}}_C} = \sqrt{(\mathbf{p} - \mathbf{q})^2}. \tag{13}$$

Remark 1. In the CGA $\mathcal{G}_{1,2+1}$ of the anti-Euclidean plane $\mathbb{R}^{0,2}$, we still have $\mathbf{e}_{\infty 1} \cdot \mathbf{e}_{o1} = -1$, and the squared distance becomes $d^2 = 2\hat{\mathbf{P}}_C \cdot \hat{\mathbf{Q}}_C$. The $\mathcal{G}_{1,3+1}$ CGA of the anti-Euclidean 3-space $\mathbb{R}^{0,3}$, called Conformal Space Algebra (CSA), is used in DCSTA [9][6] and its subalgebras CSTA and CSA. Using $\mathbb{R}^{0,2}$ is possible by just changing the signs on some results[7], like in the distance definition (13).

2.2 | 2-D CGA OPNS entities

A 2-D CGA point $\mathbf{T}_C = C(\mathbf{t})$ is on a CGA *geometric outer product null space* (OPNS) [25] plane curve entity $\mathbf{X}_C^*$ if $\mathbf{T}_C \wedge \mathbf{X}_C^* = 0$, where

$$\mathbf{X}_C^* = \mathbf{X}_C\mathbf{I}_C^{-1} \tag{14}$$

[5] In Clifford algebra, the notation $\mathcal{G}_{p,q}^k$ indicates the subset of k-vectors, i.e. all elements of grade k, $0 \le k \le (n = p + q)$, in $\mathcal{G}_{p,q}$.

[6] In standard CGA of the Euclidean plane $\mathcal{G}_{3,1}$, usually the notation for origin null vector $\mathbf{e}_o$, and for infinity null vector $\mathbf{e}_\infty$, respectively, are used. But to prepare for the TCGA notation, and to avoid confusion, we already give the notation $\mathbf{e}_{o1}$ and $\mathbf{e}_{\infty 1}$ as well.

[7] Note that in Clifford analysis [2] the m-dimensional Euclidean space is usually defined by $\mathbb{R}^{0,m}$, and the norm of a vector is then defined as $|\mathbf{p}| = \sqrt{-\mathbf{p}^2}$.

is the CGA *dual* of the CGA IPNS entity $\mathbf{X}_C$, treated in Section 2.3. An entity and its dual entity represent the same plane curve. A CGA OPNS entity can be directly formed as the wedge of up to four CGA points as

$$\mathbf{X}_C^* = \bigwedge \mathbf{P}_{C_j}, \qquad \text{for } 1 \le j \le 4, \tag{15}$$

where the $\mathbf{P}_{C_j}$ are points on the plane curve that span the plane curve. The entire plane, as a surface, can be represented by the 4-blade entity $\mathbf{I}_C$.

The CGA OPNS 3-blade *line* $\mathbf{L}_C^*$ is the wedge of two CGA points $\mathbf{P}_{C_j}$ on the line and the point $\mathbf{e}_{\infty 1}$

$$\mathbf{L}_C^* = \mathbf{P}_{C_1} \wedge \mathbf{P}_{C_2} \wedge \mathbf{e}_{\infty 1} = \mathbf{L}_C / \mathbf{I}_C \tag{16}$$

and is the CGA dual of the CGA IPNS 1-blade *line* $\mathbf{L}_C$.

The CGA OPNS 3-blade *circle* $\mathbf{C}_C^*$ is the wedge of three CGA points $\mathbf{P}_{C_j}$ on the circle

$$\mathbf{C}_C^* = \mathbf{P}_{C_1} \wedge \mathbf{P}_{C_2} \wedge \mathbf{P}_{C_3} = \mathbf{C}_C / \mathbf{I}_C \tag{17}$$

and is the CGA dual of the CGA IPNS 1-blade *circle* $\mathbf{C}_C$.

The CGA OPNS 2-blade *point pair* $\mathbf{2}_C^*$ is the wedge of two *finite* CGA points $\mathbf{P}_{C_j}$

$$\mathbf{2}_C^* = \mathbf{P}_{C_1} \wedge \mathbf{P}_{C_2} = \mathbf{2}_C / \mathbf{I}_C \tag{18}$$

and is the CGA dual[8] of the CGA IPNS 2-blade *point pair* $\mathbf{2}_C$. If one of the points is $\mathbf{e}_{\infty 1}$, then it is a CGA OPNS 2-blade *flat point* $\mathbb{P}_C^*$.

The *point pair decomposition* [3]

$$\hat{\mathbf{P}}_{C_\pm} = \frac{\mathbf{2}_C^* \mp \sqrt{\mathbf{2}_C^* \cdot \mathbf{2}_C^*}}{-\mathbf{e}_{\infty 1} \cdot \mathbf{2}_C^*} \tag{19}$$

gives the two normalized points of the point pair $\mathbf{2}_C^* = \mathbf{P}_{C_+} \wedge \mathbf{P}_{C_-}$.

The CGA OPNS 2-blade *flat point* $\mathbb{P}_C^*$ is the wedge of one *finite* CGA point $\mathbf{P}_C$ and $\mathbf{e}_{\infty 1}$

$$\mathbb{P}_C^* = \mathbf{P}_C \wedge \mathbf{e}_{\infty 1} = \mathbb{P}_C / \mathbf{I}_C \tag{20}$$

and is the CGA dual of the CGA IPNS 2-blade *flat point* $\mathbb{P}_C$. A unit scale (normalized) flat point is $\hat{\mathbb{P}}_C^* = \hat{\mathbf{P}}_C \wedge \mathbf{e}_{\infty 1}$. As explained in [3], a CGA IPNS 2-blade *flat point* $\mathbb{P}_C$ can represent the intersection of two *non-parallel* CGA IPNS 1-blade *lines* $\mathbf{L}_{C_j}$ in the plane as

$$\mathbb{P}_C^* = \mathbb{P}_C / \mathbf{I}_C = (\mathbf{L}_{C_1} \wedge \mathbf{L}_{C_2}) \mathbf{I}_C^{-1}. \tag{21}$$

The CGA *point* $\mathbf{P}_C$ of CGA OPNS 2-blade *flat point* $\mathbb{P}_C^*$ is *projected* [3] to a vector as

$$\mathbf{p}_\mathcal{E} = \mathcal{C}^{-1}(\mathbf{P}_C) = \frac{(\mathbf{e}_{o1} \wedge \mathbf{e}_{\infty 1}) \cdot (\mathbf{e}_{o1} \wedge \mathbb{P}_C^*)}{-(\mathbf{e}_{o1} \wedge \mathbf{e}_{\infty 1}) \cdot \mathbb{P}_C^*} = \frac{-\mathbb{P}_C^*}{(\mathbf{e}_{o1} \wedge \mathbf{e}_{\infty 1}) \cdot \mathbb{P}_C^*} \cdot \mathbf{e}_{o1} - \mathbf{e}_{o1}. \tag{22}$$

The null point embedding $\mathbf{P}_C = \mathcal{C}(\mathbf{p}_\mathcal{E})$, with the property $\mathbf{P}_C^2 = \mathbf{P}_C \cdot \mathbf{P}_C + \mathbf{P}_C \wedge \mathbf{P}_C = 0$, is both a CGA IPNS and OPNS point entity. There also exists the interpretation of undual IPNS 3-blade point $\mathbf{P}_C \mathbf{I}_C$.

2.3 | 2-D CGA IPNS entities

A CGA point $\mathbf{T}_C = \mathcal{C}(\mathbf{t})$ is on the CGA *geometric inner product null space* (IPNS) [25] plane curve *entity* $\mathbf{X}_C$ if $\mathbf{T}_C \cdot \mathbf{X}_C = 0$. In the two dimensions of the plane $\mathbb{R}^2$, as considered in this paper,[9] geometric entities represent plane curves and some of their intersections.

The CGA IPNS 1-blade *circle*[10] $\mathbf{C}_C$, centered at CGA point $\mathbf{P}_C = \mathcal{C}(\mathbf{p}_\mathcal{E})$ with radius r or with finite surface point $\mathbf{Q}_C$, is defined as

$$\mathbf{C}_C = \mathbf{P}_C - \frac{1}{2} r^2 \mathbf{e}_{\infty 1} = \mathbf{P}_C + \left(\mathbf{P}_C \cdot \hat{\mathbf{Q}}_C\right) \mathbf{e}_{\infty 1}. \tag{23}$$

[8] Note, that the two point pairs $\mathbf{2}_C$ and its dual $\mathbf{2}_C^*$ are orthogonal to each other. We thank the anonymous reviewers for pointing out this clarification.
[9] In three or more dimensions $\mathbb{R}^{n \ge 3}$, not considered in this paper, geometric entities more generally represent surfaces or hypersurfaces and some of their intersections.
[10] *Sphere* in $\mathbb{R}^3$.

A *normalized circle* $\hat{\mathbf{C}}_C$ has a unit scale (normalized) center point $\mathbf{P}_C = \hat{\mathbf{P}}_C$ and $\hat{\mathbf{C}}_C^2 = r^2$. The circle entity $\mathbf{C}_C$ is derived, from the constant distance $r = d(\mathbf{P}_C, \mathbf{Q}_C)$ between the finite center point $\mathbf{P}_C$ and any point $\mathbf{Q}_C$ of the circle, by the inner product test with $\mathbf{T}_C = C(\mathbf{t}_\mathcal{E})$ as

$$d^2(\mathbf{P}_C, \mathbf{Q}_C) = -2\hat{\mathbf{P}}_C \cdot \hat{\mathbf{Q}}_C = -2\hat{\mathbf{P}}_C \cdot \mathbf{T}_C = r^2, \tag{24}$$

which can be rewritten as

$$\mathbf{T}_C \cdot \hat{\mathbf{P}}_C + \frac{1}{2}r^2 = \mathbf{T}_C \cdot \left(\hat{\mathbf{P}}_C - \frac{1}{2}r^2\mathbf{e}_{\infty 1}\right) = \mathbf{T}_C \cdot \mathbf{C}_C = 0. \tag{25}$$

The CGA IPNS 1-blade *line*[11] $\mathbf{L}_C$, normal to unit vector $\hat{\mathbf{n}}_\mathcal{E}$ at distance d from the origin, or through point $\mathbf{p}_\mathcal{E}$, is defined as

$$\mathbf{L}_C = \hat{\mathbf{n}}_\mathcal{E} + d\mathbf{e}_{\infty 1} = \hat{\mathbf{n}}_\mathcal{E} + (\mathbf{p}_\mathcal{E} \cdot \hat{\mathbf{n}}_\mathcal{E})\,\mathbf{e}_{\infty 1}. \tag{26}$$

In terms of the line direction $\hat{\mathbf{d}}_\mathcal{E}$ through point $\mathbf{p}_\mathcal{E}$, where $\hat{\mathbf{d}}_\mathcal{E}^* = \hat{\mathbf{n}}_\mathcal{E} = \hat{\mathbf{d}}_\mathcal{E}\mathbf{I}_\mathcal{E}^{-1}$, the line entity can be written as

$$\mathbf{L}_C = \hat{\mathbf{d}}_\mathcal{E}^* + \left(\mathbf{p}_\mathcal{E} \cdot \hat{\mathbf{d}}_\mathcal{E}^*\right)\mathbf{e}_{\infty 1}. \tag{27}$$

The line $\mathbf{L}_C$ with unit direction $\hat{\mathbf{d}}_\mathcal{E}$ is also unit scale (normalized), where $\mathbf{L}_C = \hat{\mathbf{L}}_C$ and $\hat{\mathbf{L}}_C^2 = 1$.

In general, the wedge of $2 \le k \le 4$ CGA IPNS 1-blade entities forms a CGA IPNS k-blade entity that represents the intersection of the k 1-blade entities.

2.4 | 2-D CGA versor operations

It can be shown that reflection of point $\mathbf{P}_C$ in circle $\mathbf{C}_C$ as the versor (sandwich product) operation

$$\mathbf{P}'_C = \mathbf{C}_C\mathbf{P}_C\mathbf{C}_C^{-1} \tag{28}$$

produces $\mathbf{P}'_C$ as the *inversion* of $\mathbf{P}_C$ in the circle $\mathbf{C}_C$. The center point of circle $\mathbf{C}_C$ is $\mathbf{C}_C\mathbf{e}_{\infty 1}\mathbf{C}_C$. Successive inversions in two concentric circles, $\mathbf{C}_{C_1}$ of radius r_1 followed by $\mathbf{C}_{C_2}$ of radius r_2, produces *isotropic dilation* (uniform scaling) relative to the circle center by the factor $d = r_2^2/r_1^2$. It can also be shown that reflection of a point $\mathbf{P}_C$ in a line $\mathbf{L}_C$ as the versor operation

$$\mathbf{P}'_C = \mathbf{L}_C\mathbf{P}_C\mathbf{L}_C^{-1} \tag{29}$$

produces $\mathbf{P}'_C$ as the *reflection* of $\mathbf{P}_C$ in the line $\mathbf{L}_C$. Successive reflections in two parallel lines that are separated by a displacement $\mathbf{d}_\mathcal{E}/2$ from the first line toward the second line produces *translation* by displacement $\mathbf{d}_\mathcal{E}$. Successive reflections in two non-parallel lines subtending an angle $\theta/2$ at their intersection point from the first line toward the second line produces *rotation* by angle θ around the intersection point in the direction of the first line toward the second line.

The line entity $\mathbf{L}_C$ will also be called the *1-versor* reflection operator (*reflector*), and the circle entity $\mathbf{C}_C$ will also be called the 1-versor inversion operator (*inversor*), since they are geometric entities and also version operators (versors).

The translator (translation versor, *translat*ion operat*or*) $T = \mathbf{L}_{C_2}\mathbf{L}_{C_1} = \mathbf{L}_{C_2} \cdot \mathbf{L}_{C_1} + \mathbf{L}_{C_2} \wedge \mathbf{L}_{C_1}$ is defined as successive reflections in two parallel lines separated by half the translation displacement $\mathbf{d}_\mathcal{E}/2 = \left(\hat{\mathbf{L}}_{C_2} \wedge \hat{\mathbf{L}}_{C_1}\right) \cdot \mathbf{e}_{o1}$, or $T^2 = \mathbf{L}_{C_2}\mathbf{L}_{C_1}$ if by $\mathbf{d}_\mathcal{E}$. The rotor $R = \mathbf{L}_{C_2}\mathbf{L}_{C_1}$ is defined as successive reflections in two non-parallel lines subtending half the rotation angle $\theta/2 = \operatorname{acos}\left(\hat{\mathbf{L}}_{C_2} \cdot \hat{\mathbf{L}}_{C_1}\right)$, or $R^2 = \mathbf{L}_{C_2}\mathbf{L}_{C_1}$ if subtending θ. The isotropic dilator $D = \mathbf{C}_{C_2}\mathbf{C}_{C_1}$ is defined as successive inversions in two concentric circles with relative dilation factor $d = r_2^2/r_1^2$, or $D^2 = \mathbf{C}_{C_2}\mathbf{C}_{C_1}$ with $d^2 = r_2^2/r_1^2$. T, R, and D are called *2-versors* $V \in \{T, R, D\}$. The product of k vectors, with the product having an inverse, is called a k-versor V_k [14][13]. Their operation on a CGA entity $\mathbf{X}$ has the form $\mathbf{X}' = V\mathbf{X}V^{-1}$, called a *versor "sandwich" operation*. Each even CGA 2-versor V has an exponential form $V = \exp(\log V)$.

A *translator* is a type of versor. The CGA 2-versor *translator* T, for a translation by the displacement vector $\mathbf{d}_\mathcal{E} = d_x\mathbf{e}_1 + d_y\mathbf{e}_2$, is defined by reflections in parallel lines as

$$T = 1 + \frac{1}{2}\mathbf{e}_{\infty 1}\mathbf{d}_\mathcal{E} = \exp\left(\frac{1}{2}\mathbf{e}_{\infty 1}\mathbf{d}_\mathcal{E}\right), \tag{30}$$

where $1 = \hat{\mathbf{L}}_{C_2} \cdot \hat{\mathbf{L}}_{C_1} = \cos(0)$, and $\mathbf{e}_{\infty 1}\mathbf{d}_\mathcal{E}/2 = \hat{\mathbf{L}}_{C_2} \wedge \hat{\mathbf{L}}_{C_1}$ represents the intersection of the two parallel lines in infinity as a free vector [3] of the half displacement $\mathbf{d}_\mathcal{E}/2$.

[11] *Plane* in $\mathbb{R}^3$.

A *rotor* is a *rot*ation operat*or*. The CGA 2-versor *rotor* R, for rotation around the point $\hat{\mathbf{P}}_C = C(\mathbf{p}_\mathcal{E})$ by θ radians counter-clockwise in the right-handed xy-plane, is defined by translation of the origin rotor $\exp(\theta\mathbf{e}_2\mathbf{e}_1/2)$ by $\mathbf{d}_\mathcal{E} = \mathbf{p}_\mathcal{E}$ (i.e., $T\exp(\theta\mathbf{e}_2\mathbf{e}_1/2)\,T^{-1}$) as

$$R = \cos\left(\frac{\theta}{2}\right) + \sin\left(\frac{\theta}{2}\right)\left(\mathbf{e}_2\mathbf{e}_1 - \left(\mathbf{p}_\mathcal{E}\cdot\left(\mathbf{e}_2\mathbf{e}_1\right)\right)\mathbf{e}_{\infty 1}\right) = \cos\left(\frac{\theta}{2}\right) + \sin\left(\frac{\theta}{2}\right)\left(\hat{\mathbf{P}}_C \wedge \mathbf{e}_{\infty 1}\right)\mathbf{I}_C = \exp\left(\frac{\theta}{2}\hat{\mathbb{P}}^*_C\mathbf{I}_C\right) = \exp\left(\frac{\theta}{2}\hat{\mathbb{P}}_C\right), \quad (31)$$

where $\sin\left(\frac{\theta}{2}\right)\hat{\mathbb{P}}_C = \mathbf{L}_{C^2} \wedge \mathbf{L}_{C^1}$ is the IPNS flat point representing the intersection of the lines.

A *dilator* is a *dilat*ion operat*or*. The CGA 2-versor *isotropic dilator* D, by dilation factor $d > 0$ relative to the point $\hat{\mathbf{P}}_C = C(\mathbf{p}_\mathcal{E})$ in the plane, is defined by inversions in circles (centered on $\mathbf{p}_\mathcal{E}$ with $r_1 = 1$ and $r_2 = \sqrt{d}$) as

$$D = \frac{d+1}{2} + \frac{d-1}{2}\hat{\mathbb{P}}^*_C = \sqrt{d}\,\hat{D} = \sqrt{d}\exp\left(\operatorname{atanh}\left(\frac{d-1}{d+1}\right)\hat{\mathbb{P}}^*_C\right) = \sqrt{d}\exp\left(\frac{\ln(d)}{2}\hat{\mathbb{P}}^*_C\right), \quad (32)$$

where the exponential $\hat{D} = \exp(A)$ is a unimodular versor (n.b., $\hat{D}^\sim = \hat{D}^{-1}$) and the constant modulus (radius or invariant interval) is $\sqrt{d} = \sqrt{(d+1)^2/4 - (d-1)^2/4}$ for hyperbolic rotation by angle $\varphi = \ln(d)$ through point $((d+1)/2, (d-1)/2)$ of the hyperbolic plane. If $\hat{D}$ is used as the dilator, then the homogeneous scale on $\mathbf{e}_o$ is not preserved.

For dilation around $\mathbf{e}_o$, then $\hat{\mathbb{P}}^*_C = \mathbf{e}_o \wedge \mathbf{e}_\infty = \mathbf{e}_4\mathbf{e}_3$ and the hyperbolic rotation is in the hyperbolic Minkowski $\mathbf{e}_3\mathbf{e}_4$-plane. Then, for this rotation to form the dilation of the point $C(\mathbf{t}_\mathcal{E})$, we must have the squared versor $D^2 = \mathbf{C}_{C_2}\mathbf{C}_{C_1}$ (for $r_1 = 1, r_2 = d$, and center $\mathbf{e}_o$) as the ratio

$$\begin{aligned} D^2 &= \left(d^2\frac{\mathbf{t}^2_\mathcal{E}}{2}\mathbf{e}_{\infty 1} + \mathbf{e}_{o1}\right)\left(\frac{\mathbf{t}^2_\mathcal{E}}{2}\mathbf{e}_{\infty 1} + \mathbf{e}_{o1}\right)^{-1} \\ &= \left(\frac{d^2\mathbf{t}^2_\mathcal{E} - 1}{2}\mathbf{e}_3 + \frac{d^2\mathbf{t}^2_\mathcal{E} + 1}{2}\mathbf{e}_4\right)\left(\frac{\mathbf{t}^2_\mathcal{E} - 1}{2}\mathbf{e}_3 + \frac{\mathbf{t}^2_\mathcal{E} + 1}{2}\mathbf{e}_4\right)^{-1} \\ &= \left(\alpha'\mathbf{e}_3 + \beta'\mathbf{e}_4\right)\left(\alpha\mathbf{e}_3 + \beta\mathbf{e}_4\right)^{-1} = \frac{d^2+1}{2} + \frac{d^2-1}{2}\mathbf{e}_4\mathbf{e}_3, \end{aligned} \quad (33)$$

which can be verified after some algebra. For $r_2 = \sqrt{d}$, we get the square root $\sqrt{D^2} = D$. It can also be verified that

$$D\left(x\mathbf{e}_1 + y\mathbf{e}_2\right)D^\sim = \sqrt{d}\,\hat{D}\sqrt{d}\,\hat{D}^\sim\left(x\mathbf{e}_1 + y\mathbf{e}_2\right) = dx\mathbf{e}_1 + dy\mathbf{e}_2, \quad (34)$$

$$D^2\left(\alpha\mathbf{e}_3 + \beta\mathbf{e}_4\right) = D\left(\alpha\mathbf{e}_3 + \beta\mathbf{e}_4\right)D^\sim = \alpha'\mathbf{e}_3 + \beta'\mathbf{e}_4, \quad (35)$$

$$DC(\mathbf{t}_\mathcal{E})\,D^\sim = C\left(d\mathbf{t}_\mathcal{E}\right), \quad (36)$$

which preserves the homogeneous scale on the term $\mathbf{e}_o$. Dilation centered on $\mathbf{e}_o$ is generalized to dilation centered on a point $\mathbf{P}_C = C(\mathbf{p}_\mathcal{E})$ with the translation by $\mathbf{d}_\mathcal{E} = \mathbf{p}_\mathcal{E}$, $D' = TDT^{-1}$.

By outermorphism, all of the CGA versors operate correctly on all of the CGA OPNS entities formed as wedges of points. By dualization, the versors also work correctly on all of the CGA IPNS entities. Consider the test point[12] $\mathbf{T}_C = C(\mathbf{t}_\mathcal{E})$, an OPNS entity $\mathbf{X}^*_C$, and the outermorphism of their surface point test (their wedge) by a versor V as

$$V\left(\mathbf{T}_C \wedge \mathbf{X}^*_C\right)V^{-1} = \left(V\mathbf{T}_CV^{-1}\right) \wedge \left(V\mathbf{X}^*_CV^{-1}\right) = \mathbf{T}'_C \wedge \left(\bigwedge V\mathbf{P}_{C_j}V^{-1}\right) = \mathbf{T}'_C \wedge \mathbf{X}^{*\prime}_C. \quad (37)$$

Since the transformations of points by the versor operations (compositions of inversions in general circles $\mathbf{C}_C$, including reflections in lines $\mathbf{L}_C$) are correct, then the transformation of $\mathbf{X}^*_C$ into the entity $\mathbf{X}^{*\prime}_C$ is also correct, and the surface point test is zero only for correctly transformed surface points $\mathbf{T}'_C$. Considering the IPNS entity $\mathbf{X}_C = \mathbf{X}^*_C\mathbf{I}_C = \mathbf{X}^*_C \cdot \mathbf{I}_C$, then the test is

$$V\left(\mathbf{T}_C \cdot \left(\mathbf{X}^*_C \cdot \mathbf{I}_C\right)\right)V^{-1} = V\left(\left(\mathbf{T}_C \wedge \mathbf{X}^*_C\right)\cdot\mathbf{I}_C\right)V^{-1} = V\left(\mathbf{T}_C \wedge \mathbf{X}^*_C\right)\mathbf{I}_CV^{-1} = V\left(\mathbf{T}_C \wedge \mathbf{X}^*_C\right)V^{-1}\mathbf{I}_C. \quad (38)$$

[12] A surface in CGA is described by an outer products of points on the surface in OPNS, or the dual of this outer product in IPNS. A surface in k-CGA is described by a k-vector in IPNS. We call a conformally embedded general point *test point*, its Euclidean position is the corresponding *test vector*. In IPNS, setting to zero the inner product of a test point with a multivector representing a surface, produces an equation for all points on the surface.

3 | TRIPLE 2-D CGA $\mathcal{G}_{3(2+1),3}$ OF THE EUCLIDEAN PLANE $\mathbb{R}^2$

The Triple Conformal Geometric Algebra (TCGA) $\mathcal{T} = \mathcal{G}_{3(2+1),3}$ for the 2-D Euclidean plane $\mathbb{R}^2$ is a high-dimensional Geometric Algebra of the 12-D pseudo-Euclidean vector space $\mathbb{R}^{9,3}$. With 2^{12} basis blades, $\mathcal{T}$ is currently considered to be a high-dimensional Clifford algebra. TCGA is a staightforward extension of the concepts introduced with Double Conformal "Darboux Cyclide" Geometric Algebra (DCGA) $\mathcal{G}_{8,2}$ [10][8][7][5][4] and Double Conformal Space-Time Algebra (DCSTA) $\mathcal{G}_{4,8}$ [9][6]. Theoretically, there is no problem to similarly establish TCGA $\mathcal{G}_{12,3}$ for the 3-D Euclidean space $\mathbb{R}^3$. However, current computer algebra implementations cannot yet easily cope with elaborate computations in a high-dimensional Clifford algebra $\mathcal{G}_{12,3}$ of 2^{15} basis blades. Therefore, we pragmatically use the TCGA $\mathcal{T}$ of the Euclidean plane to explain the principles of this approach, where we only have to deal with currently feasible computations in a Clifford algebra of 2^{12} basis blades.

Triple conformal geometric algebra of the Euclidean plane $\mathcal{G}_{9,3}$ includes three copies of $\mathcal{G}_{3,1}$ CGA, which are named CGA1 $\mathcal{C}^1$, CGA2 $\mathcal{C}^2$, and CGA3 $\mathcal{C}^3$. Each CGAi $\mathcal{C}^i$ has a Euclidean plane $\mathbb{R}^2$ subalgebra $\mathcal{G}_2$, denoted $\mathcal{E}^i$.

The metric for $\mathcal{C}^1$ is $m_{\mathcal{C}^1} = \text{diag}(1,1,1,-1) = [\mathbf{e}_i \cdot \mathbf{e}_j] : i,j \in \{1,2,3,4\}$. The metric for $\mathcal{C}^2$ is $m_{\mathcal{C}^2} = \text{diag}(1,1,1,-1) = [\mathbf{e}_i \cdot \mathbf{e}_j] : i,j \in \{5,6,7,8\}$. The metric for $\mathcal{C}^3$ is $m_{\mathcal{C}^3} = \text{diag}(1,1,1,-1) = [\mathbf{e}_i \cdot \mathbf{e}_j] : i,j \in \{9,10,11,12\}$. The metric for TCGA $\mathcal{T}$ combines the metrics for $\mathcal{C}^1$, $\mathcal{C}^2$ and $\mathcal{C}^3$ as $m_{\mathcal{T}} = \text{diag}(1,1,1,-1,1,1,1,-1,1,1,1,-1) = [\mathbf{e}_i \cdot \mathbf{e}_j] : i,j \in \{1 \dots 12\}$, because together the basis vectors of $\mathcal{C}^1$, $\mathcal{C}^2$ and $\mathcal{C}^3$ span $\mathbb{R}^{9,3}$. This can be summarized as metric $m_{\mathcal{T}}$ for the 1-vectors of TCGA $\mathcal{G}^1_{9,3}$ with

$$\begin{aligned} m_{\mathcal{T}} = [m_{ij}] &= \text{diag}(1,1,1,-1,1,1,1,-1,1,1,1,-1)\,, \\ m_{ij} &= \mathbf{e}_i \cdot \mathbf{e}_j \;:\; i,j \in \{1,2,\dots,12\}. \end{aligned} \tag{39}$$

The unit pseudoscalars for $\mathcal{E}^1, \mathcal{E}^2, \mathcal{E}^3$ are $\mathbf{I}_{\mathcal{E}^1} = \mathbf{e}_1\mathbf{e}_2, \mathbf{I}_{\mathcal{E}^2} = \mathbf{e}_5\mathbf{e}_6, \mathbf{I}_{\mathcal{E}^3} = \mathbf{e}_9\mathbf{e}_{10}$, respectively, and are the dualization operators on elements $A_{\mathcal{E}^i} \in \mathcal{E}^i$ by the division $A^*_{\mathcal{E}^i} = A_{\mathcal{E}^i}/\mathbf{I}_{\mathcal{E}^i}$. Similarly, the unit pseudoscalars for $\mathcal{C}^1, \mathcal{C}^2, \mathcal{C}^3$ are $\mathbf{I}_{\mathcal{C}^1} = \mathbf{e}_1\mathbf{e}_2\mathbf{e}_3\mathbf{e}_4, \mathbf{I}_{\mathcal{C}^2} = \mathbf{e}_5\mathbf{e}_6\mathbf{e}_7\mathbf{e}_8, \mathbf{I}_{\mathcal{C}^3} = \mathbf{e}_9\mathbf{e}_{10}\mathbf{e}_{11}\mathbf{e}_{12}$, respectively, and are the dualization operators on elements $A_{\mathcal{C}^i} \in \mathcal{C}^i$ by the division $A^*_{\mathcal{C}^i} = A_{\mathcal{C}^i}/\mathbf{I}_{\mathcal{C}^i}$. The TCGA 12-blade unit pseudoscalar is $\mathbf{I}_{\mathcal{T}} = \mathbf{I}_{\mathcal{C}^1}\mathbf{I}_{\mathcal{C}^2}\mathbf{I}_{\mathcal{C}^3} = \mathbf{e}_1\mathbf{e}_2 \dots \mathbf{e}_{12}$.

In Section 2 we already discussed 2-D CGA essentially in terms of CGA1 $\mathcal{C}^1 = C$ and its Euclidean subalgebra $\mathcal{E}^1 = \mathcal{E}$ with unit vector elements $\mathbf{e}_1, \mathbf{e}_2, \mathbf{e}_3, \mathbf{e}_4$, where $\mathbf{e}_+ = \mathbf{e}_3$ and $\mathbf{e}_- = \mathbf{e}_4$. In the following subsections, we will introduce relevant multivector entities in TCGA for geometric objects and for transformation operators.

3.1 | TCGA IPNS 3-blade standard entities

The TCGA 3-blade *point* $\mathbf{P}_{\mathcal{T}}$ is the k-CGA of multiplicity $k = 3$ (TCGA) embedding

$$\mathbf{P}_{\mathcal{T}} = \mathcal{T}(\mathbf{p}_{\mathcal{E}}) = \mathcal{C}^1(\mathbf{p}_{\mathcal{E}^1})\,\mathcal{C}^2(\mathbf{p}_{\mathcal{E}^2})\,\mathcal{C}^3(\mathbf{p}_{\mathcal{E}^3}) = \mathcal{C}^1(\mathbf{p}_{\mathcal{E}^1}) \wedge \mathcal{C}^2(\mathbf{p}_{\mathcal{E}^2}) \wedge \mathcal{C}^3(\mathbf{p}_{\mathcal{E}^3})\,, \tag{40}$$

where

$$\mathcal{C}^1(\mathbf{p}_{\mathcal{E}^1}) = \mathbf{p}_{\mathcal{E}^1} + \frac{1}{2}\mathbf{p}^2_{\mathcal{E}}\mathbf{e}_{\infty 1} + \mathbf{e}_{o1}, \quad \mathcal{C}^2(\mathbf{p}_{\mathcal{E}^2}) = \mathbf{p}_{\mathcal{E}^2} + \frac{1}{2}\mathbf{p}^2_{\mathcal{E}}\mathbf{e}_{\infty 2} + \mathbf{e}_{o2}, \quad \mathcal{C}^3(\mathbf{p}_{\mathcal{E}^3}) = \mathbf{p}_{\mathcal{E}^3} + \frac{1}{2}\mathbf{p}^2_{\mathcal{E}}\mathbf{e}_{\infty 3} + \mathbf{e}_{o3}, \tag{41}$$

and

$$\mathbf{p}_{\mathcal{E}^1} = p_x\mathbf{e}_1 + p_y\mathbf{e}_2, \quad \mathbf{p}_{\mathcal{E}^2} = p_x\mathbf{e}_5 + p_y\mathbf{e}_6, \quad \mathbf{p}_{\mathcal{E}^3} = p_x\mathbf{e}_9 + p_y\mathbf{e}_{10}, \quad \mathbf{p}^2_{\mathcal{E}} = p_x^2 + p_y^2, \tag{42}$$

$$\mathbf{e}_{\infty 1} = \mathbf{e}_3 + \mathbf{e}_4, \quad \mathbf{e}_{\infty 2} = \mathbf{e}_7 + \mathbf{e}_8, \quad \mathbf{e}_{\infty 3} = \mathbf{e}_{11} + \mathbf{e}_{12}, \tag{43}$$

$$\mathbf{e}_{o1} = \frac{1}{2}(\mathbf{e}_4 - \mathbf{e}_3), \quad \mathbf{e}_{o2} = \frac{1}{2}(\mathbf{e}_8 - \mathbf{e}_7), \quad \mathbf{e}_{o3} = \frac{1}{2}(\mathbf{e}_{12} - \mathbf{e}_{11}). \tag{44}$$

The symbolic TCGA 3-blade test point $\mathbf{T}_{\mathcal{T}} = \mathcal{T}(\mathbf{t}_{\mathcal{E}})$ is the product of the embeddings of the symbolic vector $\mathbf{t}_{\mathcal{E}^1} = x\mathbf{e}_1 + y\mathbf{e}_2$ in CGA1 and its copies in CGA2 and CGA3. The scalar coefficients on all corresponding CGAi canonical basis blades are equal as copies.

Remark 2. Note that any CGAi IPNS r-blade entity $\mathbf{E}_{\mathcal{C}^i}$ has a representation as the TCGA IPNS 3r-blade entity $\mathbf{E}_{\mathcal{T}} = \mathbf{E}_{\mathcal{C}^1}\mathbf{E}_{\mathcal{C}^2}\mathbf{E}_{\mathcal{C}^3} = \mathbf{E}_{\mathcal{C}^1} \wedge \mathbf{E}_{\mathcal{C}^2} \wedge \mathbf{E}_{\mathcal{C}^3}$. If the $\mathbf{E}_{\mathcal{C}^i}$ are IPNS 1-blade entities representing an implicit curve function $F(x,y) = \mathbf{T}_{\mathcal{C}^i} \cdot \mathbf{E}_{\mathcal{C}^i} = 0$, which is a circle, line, or point, then $\mathbf{E}_{\mathcal{T}}$ represents the function $F^3(x,y) = \mathbf{T}_{\mathcal{T}} \cdot \mathbf{E}_{\mathcal{T}}$ of multiplicity 3. Therefore, we also have the TCGA IPNS 3-blade circle $\mathbf{C}_{\mathcal{T}}$ and line $\mathbf{L}_{\mathcal{T}}$ entities, and also the IPNS 3r-blade entities representing their intersections.

3.2 | TCGA IPNS 3-vector extraction operators T_s

The test point $\mathbf{T}_{\mathcal{T}}$ is a sum of $4^3 = 64$ basis 3-blades, which is a subset of the $\binom{12}{3} = 220$ canonical basis 3-blades in $\mathcal{G}_{9,3}$ TCGA. Each of the 64 3-blades has a scalar coefficient of a certain value in the variables x and y. By using each of the 64 canonical basis 3-blade reciprocals[13] as an extraction operator, each scalar coefficient can be extracted by inner product with $\mathbf{T}_{\mathcal{T}}$. Not every coefficient holds a unique value, but twenty unique values s can be extracted by certain extraction operators T_s (with index s) as $s = \mathbf{T}_{\mathcal{T}} \cdot T_s$. Together, these twenty coefficients comprise all of the available distinct coordinate polynomial coefficients $\left(x, y, x^2, xy, y^2, \ldots, \mathbf{t}_{\mathcal{E}}^6\right)$ of cubic, quartic, quintic, and sextic degrees. The extraction operators T_s are given in Tables 1, 2, and 3. For example, when expanding (40), the x-coordinate is found on three 3-blade terms: $x\left(\mathbf{e}_1\mathbf{e}_{o2}\mathbf{e}_{o3} + \mathbf{e}_{o1}\mathbf{e}_5\mathbf{e}_{o3} + \mathbf{e}_{o1}\mathbf{e}_{o2}\mathbf{e}_9\right)$. Furthermore, $-\mathbf{e}_{\infty 1}$, $-\mathbf{e}_{\infty 2}$, and $-\mathbf{e}_{\infty 3}$ are reciprocal to $\mathbf{e}_{o1}$, $\mathbf{e}_{o2}$, and $\mathbf{e}_{o3}$, respectively. Inspecting the expression for T_x in Table 1, we see that it corresponds to reversing the product order in $\left(\mathbf{e}_1\mathbf{e}_{o2}\mathbf{e}_{o3} + \mathbf{e}_{o1}\mathbf{e}_5\mathbf{e}_{o3} + \mathbf{e}_{o1}\mathbf{e}_{o2}\mathbf{e}_9\right)$, and replacing $\mathbf{e}_{oi} \leftrightarrow \mathbf{e}_{\infty i}$, $i \in \{1, 2, 3\}$, followed with division by 3, since there are three terms with x in (40). The other extraction operators in Tables 1, 2, and 3 are constructed by the same method.

Table 1. Extraction operators T_s for general quadric plane curves.

$T_x = \frac{1}{3}\left(\mathbf{e}_{\infty 3}\mathbf{e}_{\infty 2}\mathbf{e}_1 + \mathbf{e}_{\infty 3}\mathbf{e}_5\mathbf{e}_{\infty 1} + \mathbf{e}_9\mathbf{e}_{\infty 2}\mathbf{e}_{\infty 1}\right)$, $T_y = \frac{1}{3}\left(\mathbf{e}_{\infty 3}\mathbf{e}_{\infty 2}\mathbf{e}_2 + \mathbf{e}_{\infty 3}\mathbf{e}_6\mathbf{e}_{\infty 1} + \mathbf{e}_{10}\mathbf{e}_{\infty 2}\mathbf{e}_{\infty 1}\right)$
$T_{x^2} = \frac{1}{3}\left(\mathbf{e}_1\mathbf{e}_5\mathbf{e}_{\infty 3} + \mathbf{e}_1\mathbf{e}_{\infty 2}\mathbf{e}_9 + \mathbf{e}_{\infty 1}\mathbf{e}_5\mathbf{e}_9\right)$, $T_{y^2} = \frac{1}{3}\left(\mathbf{e}_2\mathbf{e}_6\mathbf{e}_{\infty 3} + \mathbf{e}_2\mathbf{e}_{\infty 2}\mathbf{e}_{10} + \mathbf{e}_{\infty 1}\mathbf{e}_6\mathbf{e}_{10}\right)$
$T_{xy} = \frac{1}{6}\left(\mathbf{e}_1\mathbf{e}_6\mathbf{e}_{\infty 3} + \mathbf{e}_2\mathbf{e}_5\mathbf{e}_{\infty 3} + \mathbf{e}_1\mathbf{e}_{\infty 2}\mathbf{e}_{10} + \mathbf{e}_2\mathbf{e}_{\infty 2}\mathbf{e}_9 + \mathbf{e}_{\infty 1}\mathbf{e}_5\mathbf{e}_{10} + \mathbf{e}_{\infty 1}\mathbf{e}_6\mathbf{e}_9\right)$
$T_1 = \mathbf{e}_\infty = \mathbf{e}_{\infty 1}\mathbf{e}_{\infty 2}\mathbf{e}_{\infty 3}$, $T_{\mathbf{t}_{\mathcal{E}}^2} = \frac{2}{3}\left(\mathbf{e}_{o1}\mathbf{e}_{\infty 2}\mathbf{e}_{\infty 3} + \mathbf{e}_{\infty 1}\mathbf{e}_{o2}\mathbf{e}_{\infty 3} + \mathbf{e}_{\infty 1}\mathbf{e}_{\infty 2}\mathbf{e}_{o3}\right)$

Table 2. Extraction operators T_s for general cubic plane curves.

$T_{x^3} = \mathbf{e}_9\mathbf{e}_5\mathbf{e}_1$, $T_{y^3} = \mathbf{e}_{10}\mathbf{e}_6\mathbf{e}_2$
$T_{xy^2} = \frac{1}{3}\left(\mathbf{e}_{10}\mathbf{e}_6\mathbf{e}_1 + \mathbf{e}_{10}\mathbf{e}_5\mathbf{e}_2 + \mathbf{e}_9\mathbf{e}_6\mathbf{e}_2\right)$, $T_{x^2y} = \frac{1}{3}\left(\mathbf{e}_{10}\mathbf{e}_5\mathbf{e}_1 + \mathbf{e}_9\mathbf{e}_6\mathbf{e}_1 + \mathbf{e}_9\mathbf{e}_5\mathbf{e}_2\right)$
$T_{x\mathbf{t}_{\mathcal{E}}^2} = \frac{1}{3}\left(\mathbf{e}_{\infty 3}\mathbf{e}_5\mathbf{e}_{o1} + \mathbf{e}_{o3}\mathbf{e}_5\mathbf{e}_{\infty 1} + \mathbf{e}_9\mathbf{e}_{\infty 2}\mathbf{e}_{o1} + \mathbf{e}_9\mathbf{e}_{o2}\mathbf{e}_{\infty 1} + \mathbf{e}_{\infty 3}\mathbf{e}_{o2}\mathbf{e}_1 + \mathbf{e}_{o3}\mathbf{e}_{\infty 2}\mathbf{e}_1\right)$
$T_{y\mathbf{t}_{\mathcal{E}}^2} = \frac{1}{3}\left(\mathbf{e}_{\infty 3}\mathbf{e}_6\mathbf{e}_{o1} + \mathbf{e}_{o3}\mathbf{e}_6\mathbf{e}_{\infty 1} + \mathbf{e}_{10}\mathbf{e}_{\infty 2}\mathbf{e}_{o1} + \mathbf{e}_{10}\mathbf{e}_{o2}\mathbf{e}_{\infty 1} + \mathbf{e}_{\infty 3}\mathbf{e}_{o2}\mathbf{e}_2 + \mathbf{e}_{o3}\mathbf{e}_{\infty 2}\mathbf{e}_2\right)$

Table 3. Extraction operators T_s for quartic, quintic, and sextic plane curves.

$T_{x^2\mathbf{t}_{\mathcal{E}}^2} = \frac{2}{3}\left(\mathbf{e}_1\mathbf{e}_5\mathbf{e}_{o3} + \mathbf{e}_1\mathbf{e}_{o2}\mathbf{e}_9 + \mathbf{e}_{o1}\mathbf{e}_5\mathbf{e}_9\right)$, $T_{y^2\mathbf{t}_{\mathcal{E}}^2} = \frac{2}{3}\left(\mathbf{e}_2\mathbf{e}_6\mathbf{e}_{o3} + \mathbf{e}_2\mathbf{e}_{o2}\mathbf{e}_{10} + \mathbf{e}_{o1}\mathbf{e}_6\mathbf{e}_{10}\right)$
$T_{xy\mathbf{t}_{\mathcal{E}}^2} = \frac{1}{3}\left(\mathbf{e}_1\mathbf{e}_6\mathbf{e}_{o3} + \mathbf{e}_2\mathbf{e}_5\mathbf{e}_{o3} + \mathbf{e}_1\mathbf{e}_{o2}\mathbf{e}_{10} + \mathbf{e}_2\mathbf{e}_{o2}\mathbf{e}_9 + \mathbf{e}_{o1}\mathbf{e}_5\mathbf{e}_{10} + \mathbf{e}_{o1}\mathbf{e}_6\mathbf{e}_9\right)$
$T_{x\mathbf{t}_{\mathcal{E}}^4} = \frac{4}{3}\left(\mathbf{e}_{o3}\mathbf{e}_{o2}\mathbf{e}_1 + \mathbf{e}_{o3}\mathbf{e}_5\mathbf{e}_{o1} + \mathbf{e}_9\mathbf{e}_{o2}\mathbf{e}_{o1}\right)$, $T_{y\mathbf{t}_{\mathcal{E}}^4} = \frac{4}{3}\left(\mathbf{e}_{o3}\mathbf{e}_{o2}\mathbf{e}_2 + \mathbf{e}_{o3}\mathbf{e}_6\mathbf{e}_{o1} + \mathbf{e}_{10}\mathbf{e}_{o2}\mathbf{e}_{o1}\right)$
$T_{\mathbf{t}_{\mathcal{E}}^4} = \frac{4}{3}\left(\mathbf{e}_{\infty 1}\mathbf{e}_{o2}\mathbf{e}_{o3} + \mathbf{e}_{o1}\mathbf{e}_{\infty 2}\mathbf{e}_{o3} + \mathbf{e}_{o1}\mathbf{e}_{o2}\mathbf{e}_{\infty 3}\right)$, $T_{\mathbf{t}_{\mathcal{E}}^6} = 8\mathbf{e}_o = 8\mathbf{e}_{o1}\mathbf{e}_{o2}\mathbf{e}_{o3}$

[13] Reciprocals may also be called pseudoinverses (see [25] and [10]).

3.3 | TCGA IPNS 3-vector entities

The most general TCGA IPNS 3-vector plane curve entity $\mathbf{\Omega}$ is a linear combination of the twenty extraction operators T_s

$$\mathbf{\Omega} = \sum_s c_s T_s. \tag{45}$$

A linear combination of extraction operators from Tables 1 and 2 forms a TCGA IPNS 3-vector general quadratic or cubic plane curve entity. A linear combination that includes the extraction operators from Table 3 can form an entity for certain types of quartic (degree 4), quintic (degree 5), and sextic (degree 6) plane curves.

The TCGA dual of any TCGA IPNS k-vector (or blade) entity $\mathbf{E}$ is its corresponding TCGA OPNS $(12-k)$-vector (or blade) entity

$$\mathbf{E}^* = \mathbf{E}\mathbf{I}_{\mathcal{T}}^{-1}, \tag{46}$$

which represents the same geometric point set or plane curve, where $\mathbf{T}_{\mathcal{T}} \wedge \mathbf{E}^* = 0$.

3.4 | TCGA IPNS intersection entities

The outer product of $2 \leq k \leq 4$ TCGA IPNS 3-blade entities forms the TCGA IPNS $3k$-blade entity that represents their intersection, which corresponds to the CGA entities but has multiplicity 3.

The outer product of any *one* TCGA IPNS 3-vector entity $\mathbf{\Omega}$ and one or two ($k \in \{1,2\}$) TCGA IPNS 3-blade entities forms the TCGA IPNS $3(k+1)$-vector entity that represents their intersection. The outer product of any two 3-vector entities (in the form of $\mathbf{\Omega}$) cannot be interpreted straightforward as intersection. Therefore, it is possible by the same method to intersect any TCGA entity with a 3-blade line or circle, but it is not possible to intersect the other general cubic and certain quadric, quintic, and sextic entities with each other. The reason for this is the general non-blade character[14] of TCGA tri-vector entities for cubic curves, and is explained in more detail in the corresponding section of [10].

3.5 | TCGA versor operations

The CGAi 1-versors $\mathbf{C}_{\mathcal{C}^i}$, $\mathbf{L}_{\mathcal{C}^i}$ and 2-versors $T_{\mathcal{C}^i}$, $R_{\mathcal{C}^i}$, and $D_{\mathcal{C}^i}$ (collectively indicated by $V_{\mathcal{C}^i}$ of grade $k \in \{1,2\}$) each have a representation as a TCGA $3k$-versor $V_{\mathcal{T}} = V_{\mathcal{C}^1} V_{\mathcal{C}^2} V_{\mathcal{C}^3}$ (the product of the same versor as represented in each CGAi). By outermorphism [25], a TCGA versor $V_{\mathcal{T}}$ operates correctly, as $\mathbf{E}' = V_{\mathcal{T}} \mathbf{E} V_{\mathcal{T}}^{-1}$, on each CGA$i$ element or factor of any TCGA IPNS entity $\mathbf{E}$ (or its OPNS dual $\mathbf{E}^*$), and therefore a TCGA versor $V_{\mathcal{T}}$ operates correctly on any TCGA entity $\mathbf{E}$.

In particular, we can rotate (by rotor $R_{\mathcal{T}} = R_{\mathcal{C}^1} R_{\mathcal{C}^2} R_{\mathcal{C}^3}$), translate ($T_{\mathcal{T}}$), and isotropically dilate ($D_{\mathcal{T}}$) any TCGA geometric entity $\mathbf{\Omega}$ for general cubic plane curves and any of the types of quartic, quintic, and sextic plane curves that can be formed as linear combinations of extraction operators T_s. For any TCGA entity $\mathbf{E}$ (which may be a quadric, cubic, etc.) and any TCGA IPNS 3-blade circle $\mathbf{C}_{\mathcal{T}}$, then $\mathbf{E}' = \mathbf{C}_{\mathcal{T}} \mathbf{E} \mathbf{C}_{\mathcal{T}}^{\sim}$ is the correct inversion of $\mathbf{E}$ in the circle $\mathbf{C}_{\mathcal{T}}$. Similarly, any TCGA entity can be reflected in the TCGA 3-blade line $\mathbf{L}_{\mathcal{T}}$.

We note, that only the use of three full copies of CGA in TCGA allows to use all conformal versor operators known from CGA. If instead only one or two copies of CGA would be used for $\mathbb{R}^2$, combined with two or one copies of GA for $\mathbb{R}^2$, then it would, e.g., not be possible to use the above translation operators for cubic plane curves, etc.

3.6 | TCGA differential operators

The extraction operators T_{x^3} and T_{y^3} are 3-blades that have inverses. This makes it possible to form the following two ratios of extraction operators

$$D_x = 3T_{x^2} T_{x^3}^{-1}, \qquad D_y = 3T_{y^2} T_{y^3}^{-1}. \tag{47}$$

Clearly, $D_x T_{x^3} = 3T_{x^2}$ and $D_y T_{y^3} = 3T_{y^2}$, such that D_x and D_y act as differential operators on the extraction operators T_s. Using the commutator product $\times$, defined for any two multivectors A and B as

$$A \times B = \frac{1}{2}(AB - BA) = -B \times A, \tag{48}$$

[14] At the moment we see no possibility to model higher degree cubic, quadric, quintic and sextic curves and surfaces by blades in k-CGA, and preserve the expressions of geometric transformations by means of versors at the same time. See the discussion in [10] and on conics in [25].

D_x and D_y produce the correct and exact derivative extraction operators $D_x \times T_s$ and $D_y \times T_s$ as shown in Tables 4, 5, and 6.

Table 4. Differential operations $D_x \times T_s$, $D_y \times T_s$ on quadric T_s of Table 1, and $\mathbf{t}_\mathcal{E} = x\mathbf{e}_1 + y\mathbf{e}_2$.

$\times$	T_x	T_y	T_{x^2}	T_{xy}	T_{y^2}	T_1	$T_{\mathbf{t}_\mathcal{E}^2}$
D_x	T_1	0	$2T_x$	T_y	0	0	$2T_x$
D_y	0	T_1	0	T_x	$2T_y$	0	$2T_y$

Table 5. Differential operations $D_x \times T_s$, $D_y \times T_s$ on cubic T_s of Table 2.

$\times$	T_{x^3}	T_{xy^2}	T_{x^2y}	T_{y^3}	$T_{x\mathbf{t}_\mathcal{E}^2}$	$T_{y\mathbf{t}_\mathcal{E}^2}$
D_x	$3T_{x^2}$	T_{y^2}	$2T_{xy}$	0	$2T_{x^2} + T_{\mathbf{t}_\mathcal{E}^2}$	$2T_{xy}$
D_y	0	$2T_{xy}$	T_{x^2}	$3T_{y^2}$	$2T_{xy}$	$2T_{y^2} + T_{\mathbf{t}_\mathcal{E}^2}$

Table 6. Differential operations $D_x \times T_s$, $D_y \times T_s$ on quartic, quintic, and sextic T_s of Table 3.

$\times$	$T_{\mathbf{t}_\mathcal{E}^4}$	$T_{x^2\mathbf{t}_\mathcal{E}^2}$	$T_{xy\mathbf{t}_\mathcal{E}^2}$	$T_{y^2\mathbf{t}_\mathcal{E}^2}$	$T_{x\mathbf{t}_\mathcal{E}^4}$	$T_{y\mathbf{t}_\mathcal{E}^4}$	$T_{\mathbf{t}_\mathcal{E}^6}$
D_x	$4T_{x\mathbf{t}_\mathcal{E}^2}$	$2T_{x^3} + 2T_{x\mathbf{t}_\mathcal{E}^2}$	$2T_{x^2y} + T_{y\mathbf{t}_\mathcal{E}^2}$	$2T_{xy^2}$	$4T_{x^2\mathbf{t}_\mathcal{E}^2} + T_{\mathbf{t}_\mathcal{E}^4}$	$4T_{xy\mathbf{t}_\mathcal{E}^2}$	$6T_{x\mathbf{t}_\mathcal{E}^4}$
D_y	$4T_{y\mathbf{t}_\mathcal{E}^2}$	$2T_{x^2y}$	$2T_{xy^2} + T_{x\mathbf{t}_\mathcal{E}^2}$	$2T_{y^3} + 2T_{y\mathbf{t}_\mathcal{E}^2}$	$4T_{xy\mathbf{t}_\mathcal{E}^2}$	$4T_{y^2\mathbf{t}_\mathcal{E}^2} + T_{\mathbf{t}_\mathcal{E}^4}$	$6T_{y\mathbf{t}_\mathcal{E}^4}$

For a unit direction $\mathbf{n} = n_x\mathbf{e}_1 + n_y\mathbf{e}_2$ in $\mathbb{R}^2$, $\mathbf{n}^2 = 1$, the $\mathbf{n}$-directional derivative operator is $D_\mathbf{n} = n_x D_x + n_y D_y$ and the $\mathbf{n}$-directional derivative of any TCGA IPNS 3-vector entity $\mathbf{\Omega}$ representing an implicit plane curve function $F(x, y) = \mathbf{T}_\mathcal{T} \cdot \mathbf{\Omega}$ is $\partial_\mathbf{n}\mathbf{\Omega} = D_\mathbf{n} \times \mathbf{\Omega}$, which represents the implicit plane curve function $\partial_\mathbf{n} F = (\boldsymbol{\nabla} \cdot \mathbf{n})\, F = \mathbf{T}_\mathcal{T} \cdot \left(D_\mathbf{n} \times \mathbf{\Omega}\right)$, where the gradient operator is the geometric calculus symbolic vector $\boldsymbol{\nabla} = (\partial/\partial x)\,\mathbf{e}_1 + (\partial/\partial y)\,\mathbf{e}_2$. For a TCGA IPNS 3-blade 3-CGA entity $\mathbf{C}_\mathcal{T}$, which represents the third power[15] of a function $F^3(x, y) = F(x, y)\, F(x, y)\, F(x, y)$, the product $\mathbf{T}_\mathcal{T} \cdot \left(D_x \times \mathbf{C}_\mathcal{T}\right) = 3F^2\partial_x F$ etc., which is in agreement with the chain rule of differentiation. Mixed partial derivatives of higher orders are formed by nesting successive differential operations in any sequence (e.g., $D_y \times \left(D_x \times \mathbf{\Omega}\right)$ or $D_x \times \left(D_y \times \mathbf{\Omega}\right)$), etc.

3.7 | Examples of plane curve TCGA 3-vector entities

The TCGA plane curves are represented in algebraic geometry by implicit plane curve functions $F(x, y)$, with equation $F(x, y) = 0$, that have a straightforward representation as TCGA entities (i.e., as linear combinations of the extraction operators in Tables 1, 2, and 3), as will be shown in the following subsections. Points of a plane curve are solutions of the implicit equation $F(x, y) = 0$, equivalent to the inner product null space of a TCGA IPNS 3-vector plane curve entity $\mathbf{\Omega}$ (i.e., points $\mathbf{P}_\mathcal{T}$ where $\mathbf{P}_\mathcal{T} \cdot \mathbf{\Omega} = 0$). Many functions $F(x, y)$ include some real scalar parameters a, b, and c that vary the curve.

An exhaustive description of all possible linear, quadric, cubic, quartic, quintic, and sextic plane curves that can be represented as TCGA IPNS 3-vector entities would be beyond the limits of this introductory paper. The current subsection instead presents some examples of TCGA IPNS 3-vector entities for some of the plane curves commonly discussed in algebraic geometry literature.

[15] The third power arises, because we use three copies of CGA to produce TCGA.

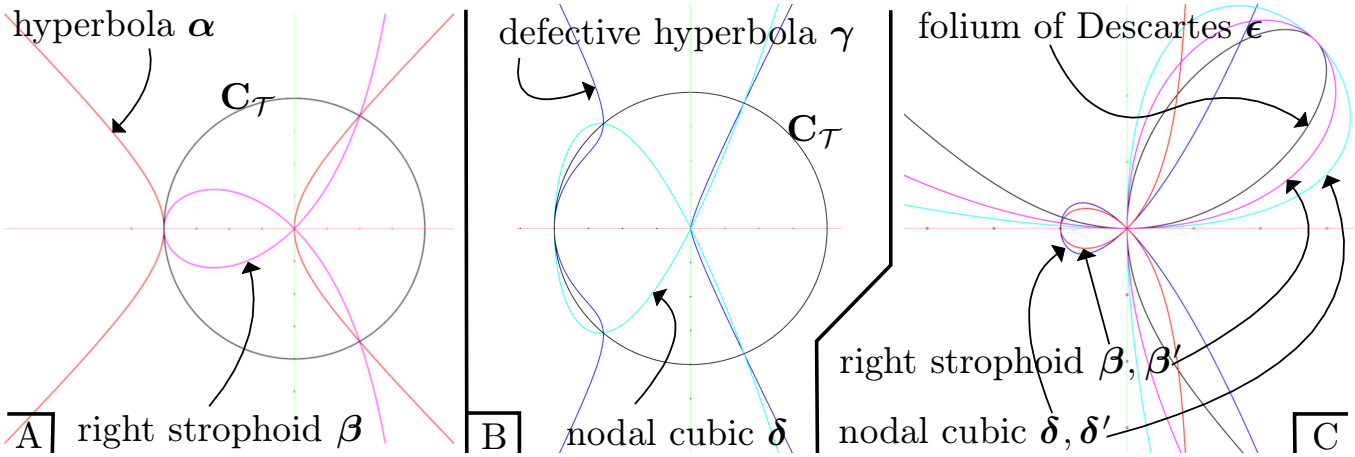

Figure 1. Examples of cubics: right strophoid, nodal cubic, and folium of Descartes.

3.7.1 | General cubic plane curves

TCGA IPNS 3-vector entities can represent general cubic (degree 3) plane curves as linear combinations of the general quadric (degree 2) and general cubic extraction operators listed in Tables 1 and 2. In algebraic geometry, references [24] and [12] contain numerous implicit cubic plane curve equations $F(x, y) = 0$, all of which can be represented as TCGA IPNS 3-vector entities. Examples of TCGA cubic plane curve entities are shown in Table 7.

Table 7. Examples of TCGA IPNS 3-vector *cubic* plane curve entities.

Name	Cubic $F(x, y)$	TCGA IPNS 3-vector entity
Apollonian cubic	$(x-a)\left(x^2+y^2\right)+bx+cy$	$T_{x\mathbf{t}_\mathcal{E}^2} - aT_{\mathbf{t}_\mathcal{E}^2} + bT_x + cT_y$
cissiod of Diocles	$x^3+xy^2-y^2$	$T_{x^3} + T_{xy^2} - T_{y^2}$
cubic egg	$axy^2+x^2+y^2-1$	$aT_{xy^2} + T_{\mathbf{t}_\mathcal{E}^2} - T_1$
egg of Newton	$y^2-x^3+ax^2+x-a$	$T_{y^2} - T_{x^3} + aT_{x^2} + T_x - aT_1$
folium of Descartes	$x^3+y^3-\sqrt{2}axy$	$T_{x^3} + T_{y^3} - \sqrt{2}aT_{xy}$
nodal cubic	$y^2-x^2(x-a) : a<0$	$T_{y^2} - T_{x^3} + aT_{x^2}$
serpentine	x^2y+a^2y-abx	$T_{x^2y} + a^2T_y - abT_x$
right strophoid	$y^2(x+a)+x^2(x-a)$	$T_{xy^2} + aT_{y^2} + T_{x^3} - aT_{x^2}$
trident of Newton	$xy-x^3-ax^2-bx-c$	$T_{xy} - T_{x^3} - aT_{x^2} - bT_x - cT_1$
witch of Agnesi	$x^2y+4a^2y-8a^3$	$T_{x^2y} + 4a^2T_y - 8a^3T_1$

Figure 1 (A) shows the inversion of the quadric hyperbola $\boldsymbol{\alpha}$ in the circle $\mathbf{C}_\mathcal{T}$ as the cubic right strophoid $\boldsymbol{\beta} = \mathbf{C}_\mathcal{T}\boldsymbol{\alpha}\mathbf{C}_\mathcal{T}^\sim$ for $a = -4$. The hyperbola entity $\boldsymbol{\alpha} = T_\mathcal{T}\left(T_{x^2} - T_{y^2} - r^2T_1\right)T_\mathcal{T}^\sim$ has radius $r = 2$ and is translated by displacement $\mathbf{d}_\mathcal{E} = -r\mathbf{e}_1$ using the TCGA translator $T_\mathcal{T}$. The TCGA IPNS 3-blade circle $\mathbf{C}_\mathcal{T}$ has radius $r = 4$ and center $\mathbf{e}_o$ (the origin). The right strophoid $\boldsymbol{\beta}$ is an entity that can also be represented in Double Conformal Geometric Algebra (DCGA) [5].

Figure 1 (B) shows the inversion of the nodal cubic $\boldsymbol{\delta}$ for $a = -4$ in the circle $\mathbf{C}_\mathcal{T}$ (of radius $r = 4$ centered on $\mathbf{e}_o$) as the quartic "defective hyperbola" $\boldsymbol{\gamma}$ for $a = -4$ (see quartics Table 8).

Figure 1 (C) shows a right strophoid $\boldsymbol{\beta}$ and nodal cubic $\boldsymbol{\delta}$, both for $a = -1$, which are both dilated by factor $d = 4$ and rotated by angle $\theta = 225°$ using the TCGA dilator $D_\mathcal{T}$ and rotor $R_\mathcal{T}$ as $\boldsymbol{\beta}' = R_\mathcal{T}D_\mathcal{T}\boldsymbol{\beta}D_\mathcal{T}^\sim R_\mathcal{T}^\sim$ and $\boldsymbol{\delta}' = R_\mathcal{T}D_\mathcal{T}\boldsymbol{\delta}D_\mathcal{T}^\sim R_\mathcal{T}^\sim$. The right

strophoid $\boldsymbol{\beta}'$ and nodal cubic $\boldsymbol{\delta}'$ both look similar to a folium of Descartes. However, the true folium of Descartes $\boldsymbol{\epsilon}$ for $a = 4$ is also shown, and the shape differences are apparent.

By using TCGA entities and versor operations, it is easy to use TCGA as a tool to study the plane curves of Figure 1, and many others, and to learn how plane curves are related to each other through inversions in circles and by rotations, dilations, and translations.

3.7.2 | Various quartic plane curves

TCGA IPNS 3-vector entities can represent only the specific forms of quartic (degree 4) plane curves that can be written in terms of the general cubic extraction operators (all of Tables 1 and 2) plus the available quartic extraction operators of Table 3, which can represent only the quartic terms $\mathbf{t}_\mathcal{E}^4$, $x^2\mathbf{t}_\mathcal{E}^2$, $xy\mathbf{t}_\mathcal{E}^2$, and $y^2\mathbf{t}_\mathcal{E}^2$, where $\mathbf{t}_\mathcal{E}^2 = x^2 + y^2$. TCGA *cannot* represent the individual general quartic terms x^4, x^2y^2, and y^4 with independent coefficients, because there are no extraction trivector operators to individually extract these coefficients from a general test point. Even with this limitation, there is a large variety of quartics in the algebraic geometry literature (e.g., in [24]) that can be written with this restricted choice of TCGA quartic terms. Some of the possible TCGA quartic plane curve entities are shown in Table 8.

Table 8. Examples of TCGA IPNS 3-vector *quartic* plane curve entities.

Name	TCGA IPNS 3-vector quartic entity
cardioid	$T_{\mathbf{t}_\mathcal{E}^4} - 4aT_{x\mathbf{t}_\mathcal{E}^2} + 4a^2T_{x^2} - 4a^2T_{\mathbf{t}_\mathcal{E}^2}$
Cartesian oval	$b^2\left(T_{\mathbf{t}_\mathcal{E}^4} + 2a^2T_{\mathbf{t}_\mathcal{E}^2} + a^4T_1\right) - 4abc\left(T_{x\mathbf{t}_\mathcal{E}^2} + a^2T_x\right) + 4a^2c^2T_{x^2} - 2c\left(T_{\mathbf{t}_\mathcal{E}^2} + a^2T_1\right) + 4abT_x + T_1$
Cassini oval	$T_{\mathbf{t}_\mathcal{E}^4} - 2a^2\left(T_{x^2} - T_{y^2}\right) + \left(a^4 - b^4\right)T_1$
conchoid of Durer	$2T_{y^2\mathbf{t}_\mathcal{E}^2} - 2b\left(T_{xy^2} + T_{y^3}\right) + \left(b^2 - 3a^2\right)T_{y^2} - a^2T_{x^2} + 2a^2b\left(T_x + T_y\right) + a^2\left(a^2 - b^2\right)T_1$
conchoid of Nicomedes	$T_{x^2\mathbf{t}_\mathcal{E}^2} - 2bT_{x\mathbf{t}_\mathcal{E}^2} + b^2T_{\mathbf{t}_\mathcal{E}^2} - a^2T_{x^2}$
defective hyperbola	$aT_{x^2\mathbf{t}_\mathcal{E}^2} + T_{y^2\mathbf{t}_\mathcal{E}^2} - a^2T_{x^3} : a < 0$
deltoid (tricuspid)	$T_{\mathbf{t}_\mathcal{E}^4} - 8a\left(T_{x^3} - 3T_{xy^2}\right) + 18a^2T_{\mathbf{t}_\mathcal{E}^2} - 27a^4T_1$
hippopede	$T_{\mathbf{t}_\mathcal{E}^4} + 4b(b-a)T_{\mathbf{t}_\mathcal{E}^2} - 4b^2T_{x^2}$
kappa	$T_{y^2\mathbf{t}_\mathcal{E}^2} - a^2T_{x^2}$
limacon	$T_{\mathbf{t}_\mathcal{E}^4} - 4aT_{x\mathbf{t}_\mathcal{E}^2} + 4a^2T_{x^2} - b^2T_{\mathbf{t}_\mathcal{E}^2}$
ovoid	$aT_{x^2\mathbf{t}_\mathcal{E}^2} + T_{y^2\mathbf{t}_\mathcal{E}^2} - a^2T_{x^3} : a > 0$

A type of hippopede $\mathbf{H}$ can be formed as the inversion $\mathbf{H} = \mathbf{C}_\mathcal{T}\mathbf{E}\mathbf{C}_\mathcal{T}^\sim$ of an ellipse $\mathbf{E} = T_{x^2}/a^2 + T_{y^2}/b^2 - T_1$, $a>b$, in the circle $\mathbf{C}_\mathcal{T}$ of radius $r = b$ centered on $\mathbf{e}_o$. $\mathbf{H}$ has y-intercepts $\pm b$ and x-intercepts $\pm c = b^2/a$ (the inversion of $\pm a$). For fixed b, then $a = b^2/c$ gives $\mathbf{H}$ with x,y-intercepts $\pm c, \pm b$. As $a \to \infty$ for fixed b, $\mathbf{E} = T_{y^2}/b^2 - T_1$ and $\mathbf{H}$ becomes a particular *lemniscate of Booth* (figure eight) that is the union of tangential spheres of radius b through the origin. The implicit curve function $F(x, y) = \mathbf{T}_\mathcal{T} \cdot \mathbf{H}$ has a factor $\mathbf{t}_\mathcal{E}^2 = x^2 + y^2$ (making it appear sextic) representing the inversion $\mathbf{e}_o = \mathbf{C}_\mathcal{T}\mathbf{e}_\infty\mathbf{C}_\mathcal{T}^\sim$ since all entities, such as $\mathbf{E}$, not having the term $T_{\mathbf{t}_\mathcal{E}^6} = 8\mathbf{e}_o$ include $\mathbf{e}_\infty$ as a singular outlier *handle point* (exterior point). $F(x, y)/\mathbf{t}_\mathcal{E}^2$ is the quartic hippopede function.

Many of the quartics of Table 8, including $\mathbf{H}$ and hippopede, can also be formed in DCGA [5].

Figure 2 shows the hippopede $\mathbf{H}$ that has been discussed above and also a cardioid, Cartesian oval, and deltoid. The larger cardioid, call it $\mathbf{A}$, with a=1, was rotated $\theta = -90°$, then dilated by $d = 1/2$, and then translated by $\mathbf{d}_\mathcal{E} = 2\mathbf{e}_1$ into the smaller cardioid $\mathbf{A}' = T_\mathcal{T}D_\mathcal{T}R_\mathcal{T}\mathbf{A}R_\mathcal{T}^\sim D_\mathcal{T}^\sim T_\mathcal{T}^\sim$. The Cartesian oval and the deltoid were both reflected in the circle (inversion in circle).

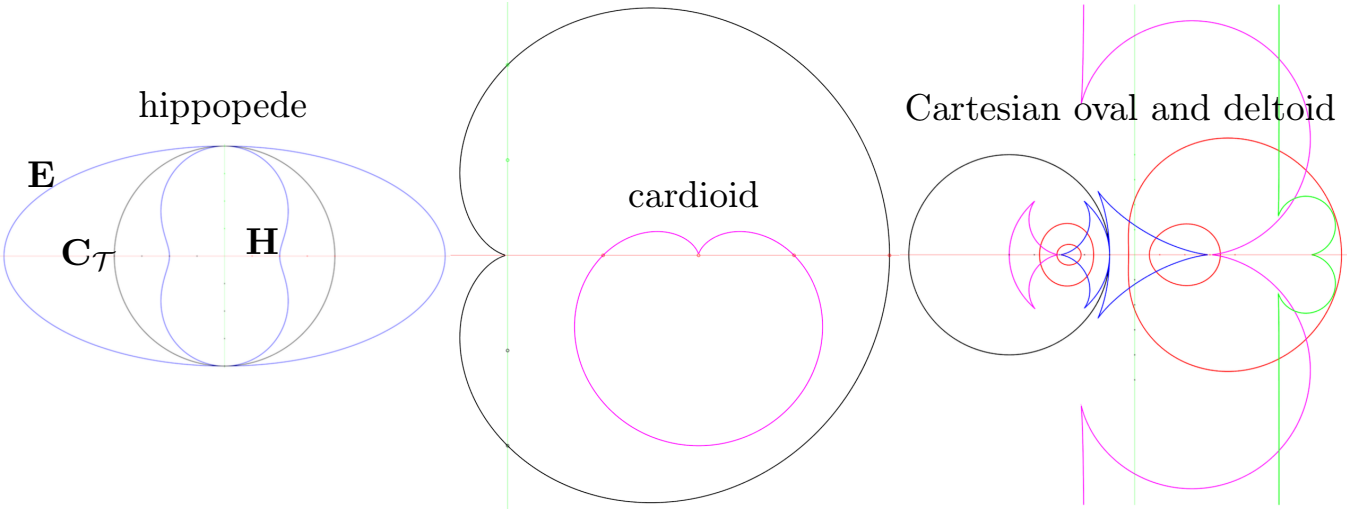

Figure 2. Examples of quartics: the hippopede, cardioid, Cartesian oval, and deltoid.

The reflected deltoid makes a shape that looks similar to an axe head, which is then rotated 180° and then reflected again in the circle to make the larger B-like shape. The larger B-like shape is then dilated by $d = 1/4$ (centered on $3\mathbf{e}_1$) and translated by $\mathbf{d}_{\mathcal{E}} = 4\mathbf{e}_1$ to make the smaller B-like shape.

3.7.3 | Various quintic plane curves

In Table 3, we find that TCGA offers only two quintic (degree 5) extraction operators that can represent only the quintic terms $x\mathbf{t}_{\mathcal{E}}^4$ and $y\mathbf{t}_{\mathcal{E}}^4$, where $\mathbf{t}_{\mathcal{E}}^2 = x^2 + y^2$. This may seem limited, but in combination with all of the quartic and lesser degree terms available in TCGA, there is still a large variety of possible TCGA IPNS 3-vector quintic plane curve entities. The literature on quintic plane curves appears sparse, so we have only a couple of ad-hoc examples in Table 9.

Table 9. Examples of TCGA IPNS 3-vector *quintic* plane curve entities.

Description	TCGA IPNS 3-vector quintic entity
modified Burnside curve	$T_{y^2} - T_{x\mathbf{t}_{\mathcal{E}}^4} + T_x$
serpentine-like	$T_{x\mathbf{t}_{\mathcal{E}}^4} - T_{x^3} - T_{y^3}/125 - \left(T_{x^2} + T_{y^2}\right)/144 + \left(T_x + T_y\right)/100$

3.7.4 | Cranioid sextic plane curves

A sextic (degree 6) *cranioid* (head-like shape) plane curve can be formed by inversion in a circle of a cubic curve that is basically a straight line except for being curved as it passes through the origin (see Figure 3). Such a cubic curve is

$$y - b + \frac{b}{x^2 + 1} = 0. \tag{49}$$

As $x \to \infty$, it becomes the line $y = b$. As $x \to 0$, then $y \to 0$. The function is of even degree 2 in x and symmetrical for $\pm x$. After multiplying by $x^2 + 1$, the TCGA IPNS 3-vector entity $\mathbf{B}_0$ for this cubic plane curve can be directly expressed in terms of the TCGA IPNS extraction operators as

$$\mathbf{B}_0 = T_{x^2 y} + T_y - bT_{x^2}. \tag{50}$$

We will use $b = -1$, such that the curvature is upwards the y-axis. Instead of using x^2, we can use $\mathbf{t}_{\mathcal{E}}^4 = \left(x\mathbf{e}_1 + y\mathbf{e}_2\right)^4 = \left(x^2 + y^2\right)^2$ for a sharper curvature. The TCGA IPNS 3-vector entity $\mathbf{B}_1$ for this quintic plane curve is

$$\mathbf{B}_1 = T_{y\mathbf{t}_{\mathcal{E}}^4} + T_y - bT_{\mathbf{t}_{\mathcal{E}}^4}. \tag{51}$$

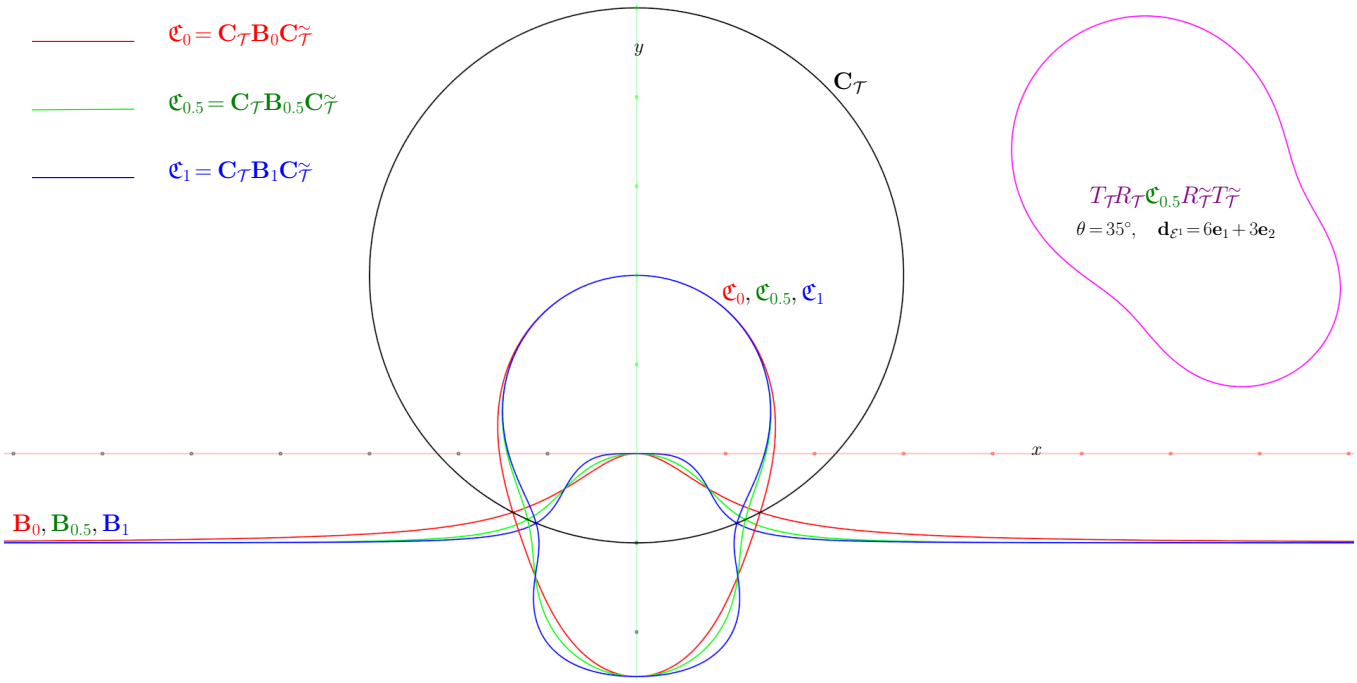

Figure 3. Cranioids $\mathfrak{C}_0$, $\mathfrak{C}_{0.5}$, and $\mathfrak{C}_1$.

The TCGA IPNS 3-vector entity $\mathbf{B}_t$, $0 \le t \le 1$, that interpolates between $\mathbf{B}_0$ and $\mathbf{B}_1$ is

$$\mathbf{B}_t = (1-t)\,\mathbf{B}_0 + t\mathbf{B}_1. \tag{52}$$

Using the TCGA IPNS 3-blade circle $\mathbf{C}_\mathcal{T} = \mathbf{C}_{\mathcal{C}^1}\mathbf{C}_{\mathcal{C}^2}\mathbf{C}_{\mathcal{C}^3}$ with center $2\mathbf{e}_2$ and radius $r = 3$, and $\mathbf{B}_t$ with parameters $0 \le t \le 1$ and $b = -1$, the TCGA IPNS 3-vector *cranioid* entity $\mathfrak{C}_t$ is the inversion

$$\mathfrak{C}_t = \mathbf{C}_\mathcal{T}\mathbf{B}_t\mathbf{C}_\mathcal{T}^\sim. \tag{53}$$

For $t < 0$ and $t > 1$, the entity $\mathfrak{C}_t$ is generally no longer a cranioid but forms other interesting curves. Choosing a different b for the curve $\mathbf{B}_t$ and different circles $\mathbf{C}_\mathcal{T}$ for the inversion could be the subject of further experimentation. Further research could also lead to various ways to parametrize the cranioid entity for certain shapes.

Figure 3 shows three cranioids $\mathfrak{C}_0$, $\mathfrak{C}_{0.5}$, and $\mathfrak{C}_1$, and it also shows a cranioid $\mathfrak{C}'_{0.5} = T_\mathcal{T}R_\mathcal{T}\mathfrak{C}_{0.5}R_\mathcal{T}^\sim T_\mathcal{T}^\sim$ that has been rotated 35° using a TCGA rotor $R_\mathcal{T}$ and then translated by $\mathbf{d}_{\mathcal{E}^1} = 6\mathbf{e}_1 + 3\mathbf{e}_2$ using a TCGA translator $T_\mathcal{T}$.

Cayley's sextic, with equation $4\left(x^2+y^2-ax\right)^3 = 27a^2\left(x^2+y^2\right)^2$, can also be represented as a TCGA entity.

3.8 | The anisotropic dilation operation

A TCGA 3-vector *general cubic* entity $\mathbf{X}_\mathcal{T}$ (a linear combination of extraction operators from Tables 1 and 2) can represent *any* cubic plane curve, including those that have been anisotropically dilated by a factor $d > 0$ in an arbitrary direction $\hat{\mathbf{d}}_\mathcal{E}$ (directed scaling). The TCGA 6-versor dilator $D_\mathcal{T}$ is only for isotropic dilation (uniform scaling), and we have not been able to give an anisotropic dilation versor in $\mathcal{G}_{9,3}$ TCGA. However, the following describes a successful extension of TCGA in which we can obtain an anisotropic dilation versor $B_\mathcal{T}$ that is valid on any general TCGA cubic entity $\mathbf{X}_\mathcal{T}$.

TCGA can be generalized further by adding[16] three new unit vector elements $[\mathbf{e}_i \cdot \mathbf{e}_j] = [m_{ij}] = \text{diag}(-1,-1,-1) : i,j \in \{13,14,15\}$ as time-like dimensions, forming a triple of Minkowski space-times $\mathcal{M}^i : i \in \{1,2,3\}$ of signatures $(2,1)$, each having two space dimensions and a time-like dimension. In this new space-time, vectors are written[17] as $\mathbf{t}_{\mathcal{M}^1} = x\mathbf{e}_1 + y\mathbf{e}_2 + w\mathbf{e}_{13}$, and similarly for $\mathbf{t}_{\mathcal{M}^2}$ and $\mathbf{t}_{\mathcal{M}^3}$ using $\mathbf{e}_{14}$ and $\mathbf{e}_{15}$, respectively. We still have Euclidean spatial vectors $\mathbf{t}_{\mathcal{E}^1} = x\mathbf{e}_1 + y\mathbf{e}_2$, and similarly for $\mathbf{t}_{\mathcal{E}^2}$ and $\mathbf{t}_{\mathcal{E}^3}$, as previously defined. The new time-like coordinate w can be written $w = ct$, with light speed $c = 1$

[16] Please note, that this increase in dimension may lead to a substantial increase in computation time, when compared to TCGA for the Euclidean plane in $\mathcal{G}_{9,3}$.
[17] Note, that the indexes 13, 14, and 15 do not indicate bivectors, but rather enumerate vectors.

and time t. In this larger $\mathcal{G}_{3(2+1),3(1+1)}$ 15-D algebra, which is less practicable[18], it becomes now possible to define the unimodular hyperbolic rotor (*boost*[19] versor) $B_{\mathcal{M}^1} = \exp\left(\varphi_d \hat{\mathbf{d}}_{\mathcal{E}^1} \mathbf{e}_{13}/2\right)$ for *anisotropic dilation* in direction $\hat{\mathbf{d}}_{\mathcal{E}^1}$ by dilation factor $d > 0$, with hyperbolic angle (rapidity) $\varphi_d = \operatorname{atanh}(-\beta_d)$ and natural speed $\beta_d = \sqrt{1-d^2}$, in accordance with the length L_0 contraction $L = dL_0 = \gamma_d^{-1} L_0 = \sqrt{1-\beta_d^2} L_0$ that is well-known in physics as part of the theory of special relativity. Note that, β_d and φ_d are imaginary numbers for dilation factor $d>1$, and then (just for this anisotropic dilation operation) we must use the triple conformal Clifford algebra $C\ell(3(2+1), 3(1+1))$ for the complex vector space $\mathbb{C}^{2,1}$. Also note that, the rotation would be by the negative angle $-\varphi_d$ in the other Minkowski spacetimes with signatures $(1,2)$. The boost versor $B_{\mathcal{M}^1}$ corresponds to a space-time boost *from* the stationary observer space-time velocity vector $\mathbf{o}_{\mathcal{M}^1} = c\mathbf{e}_{13}$ *into* the space-time velocity vector $\gamma_d \mathbf{d}_{\mathcal{M}^1} = \gamma_d(\beta_d c \hat{\mathbf{d}}_{\mathcal{E}^1} + c\mathbf{e}_{13})$, where

$$\mathbf{d}_{\mathcal{M}^1} = \beta_d c \hat{\mathbf{d}}_{\mathcal{E}^1} + c\mathbf{e}_{13}, \quad \mathbf{o}_{\mathcal{M}^1} = c\mathbf{e}_{13}, \quad \mathbf{o}_{\mathcal{M}^1}^{-1} = -\mathbf{e}_{13}/c, \tag{54}$$

$$H = \mathbf{d}_{\mathcal{M}^1}/\mathbf{o}_{\mathcal{M}^1} = 1 - \beta_d \hat{\mathbf{d}}_{\mathcal{E}^1} \mathbf{e}_{13}, \quad |H| = \sqrt{1^2 - \beta_d^2} = \gamma_d^{-1}, \quad \varphi_d = \operatorname{atanh}(-\beta_d), \tag{55}$$

$$\hat{H} = \cosh(\varphi_d) + \sinh(\varphi_d)\hat{\mathbf{d}}_{\mathcal{E}^1}\mathbf{e}_{13} = \exp(\varphi_d \hat{\mathbf{d}}_{\mathcal{E}^1}\mathbf{e}_{13}) = |H|^{-1} H = \gamma_d H, \tag{56}$$

$$B_{\mathcal{M}^1} = \sqrt{\hat{H}} = \sqrt{\gamma_d H} = \sqrt{\gamma_d \mathbf{d}_{\mathcal{M}^1} \mathbf{o}_{\mathcal{M}^1}^{-1}} = \exp(\varphi_d \hat{\mathbf{d}}_{\mathcal{E}^1}\mathbf{e}_{13}/2), \quad B_{\mathcal{M}^1}^2 = \gamma_d H, \tag{57}$$

$$\gamma_d \mathbf{d}_{\mathcal{M}^1} = B_{\mathcal{M}^1}^2 \mathbf{o}_{\mathcal{M}^1} = B_{\mathcal{M}^1} \mathbf{o}_{\mathcal{M}^1} B_{\mathcal{M}^1}^{\sim}. \tag{58}$$

Similarly, we have the hyperbolic rotors in $\mathcal{M}^2$ and $\mathcal{M}^3$ as

$$B_{\mathcal{M}^2} = \exp(\varphi_d \hat{\mathbf{d}}_{\mathcal{E}^2}\mathbf{e}_{14}/2), \quad B_{\mathcal{M}^3} = \exp(\varphi_d \hat{\mathbf{d}}_{\mathcal{E}^3}\mathbf{e}_{15}/2). \tag{59}$$

The triple hyperbolic rotor is $B_{\mathcal{T}} = B_{\mathcal{M}^1} B_{\mathcal{M}^2} B_{\mathcal{M}^3}$. If we hold $w = 0$, then the 15-D $\mathcal{G}_{9,6}$ algebra, denoted $\mathcal{TM}$, reduces to the 12-D $\mathcal{G}_{9,3}$ TCGA $\mathcal{T}$. In effect, we can set $w = 0$ in any entity $\mathbf{X}_{\mathcal{TM}}$ in $\mathcal{TM}$ by the projection

$$\mathbf{X}'_{\mathcal{T}} = (\mathbf{X}_{\mathcal{TM}} \cdot \mathbf{I}_{\mathcal{T}})\mathbf{I}_{\mathcal{T}}^{-1} = \mathcal{P}_{\mathbf{I}_{\mathcal{T}}}(\mathbf{X}_{\mathcal{TM}}). \tag{60}$$

The anisotropic dilation, centered on (relative to) the origin $\mathbf{e}_o$ and in the direction $\hat{\mathbf{d}}_{\mathcal{E}}$ by dilation factor $d > 0$, of any TCGA IPNS 3-vector *cubic* entity $\mathbf{X}_{\mathcal{T}}$ is defined as

$$\mathbf{X}'_{\mathcal{T}} = \mathcal{P}_{\mathbf{I}_{\mathcal{T}}}(B_{\mathcal{T}} \mathbf{X}_{\mathcal{T}} B_{\mathcal{T}}^{\sim}) = \mathcal{P}_{\mathbf{I}_{\mathcal{T}}}(\mathbf{X}_{\mathcal{TM}}). \tag{61}$$

A translated boost versor $B_{\mathcal{T}}^{\mathbf{p}} = T_{\mathcal{T}} B_{\mathcal{T}} T_{\mathcal{T}}^{\sim}$, with translator $T_{\mathcal{T}}$ for displacement $\mathbf{p}_{\mathcal{E}}$, creates a boost versor $B_{\mathcal{T}}^{\mathbf{p}}$ for anisotropic dilation centered on $\mathbf{p}_{\mathcal{E}}$. The boost $\mathbf{X}_{\mathcal{TM}} = B_{\mathcal{T}}^{\mathbf{p}} \mathbf{X}_{\mathcal{T}} (B_{\mathcal{T}}^{\mathbf{p}})^{\sim}$ of a cubic entity $\mathbf{X}_{\mathcal{T}}$ that is centered on $\mathbf{p}_{\mathcal{E}}$ is set into the constant velocity $\mathbf{v}_{\mathcal{E}} = \beta_d c \hat{\mathbf{d}}_{\mathcal{E}}$ of the boost, where $\mathbf{X}_{\mathcal{TM}}$ is centered at $\mathbf{p}_{\mathcal{E}} + \mathbf{v}_{\mathcal{E}} t$ at time t, and the shape of $\mathbf{X}_{\mathcal{TM}}$ and $\mathbf{X}'_{\mathcal{T}}$ is contracted (or dilated) in direction $\hat{\mathbf{d}}_{\mathcal{E}}$ by the factor $d = \sqrt{1-\beta_d^2}$. The projection back to a general TCGA IPNS 3-vector cubic entity $\mathbf{X}'_{\mathcal{T}} = \mathcal{P}_{\mathbf{I}_{\mathcal{T}}}(\mathbf{X}_{\mathcal{TM}})$ is at $w = ct = 0$ and centered at its original center $\mathbf{p}_{\mathcal{E}}$ (or whatever it was before the boost), but its shape retains the $\hat{\mathbf{d}}_{\mathcal{E}}$-directional dilation by dilation factor d away from the chosen center $\mathbf{p}_{\mathcal{E}}$.

Only the general cubic entities support a form, in terms of the TCGA extraction elements, that can be anisotropically dilated, and any attempt to anisotropically dilate other TCGA entities of degrees 4, 5, or 6 (quartic, quintic, sextic) will result in a different kind of transformation of the shape of the entity.

The anisotropic dilation operation only requires the inclusion of the vector units $\mathbf{e}_{13}$, $\mathbf{e}_{14}$, and $\mathbf{e}_{15}$, the ability of the algebra to use complex number scalars, and the versor $B_{\mathcal{T}}^{\mathbf{p}}$ and projection $\mathcal{P}_{\mathbf{I}_{\mathcal{T}}}(\mathbf{X}_{\mathcal{TM}})$. No other changes or additions are required to TCGA, including no changes are required to the TCGA point entity or other TCGA entities and versors.

Finally, Figure 4 shows an example for directed (anisotropic) scaling of the folium of Descartes, with $a = 1$, dilated by $d = 5$ in the diagonal direction $\mathbf{e}_1 + \mathbf{e}_2$.

[18] The notion of *less practicable* only refers to the higher computational cost due to the increase in dimensions of the Clifford algebra thus generated.

[19] The term *boost* is taken over from special relativity, but the hyperbolic rotor we use currently only serves as anisotropic dilation operator for the purpose of shape manipulation.

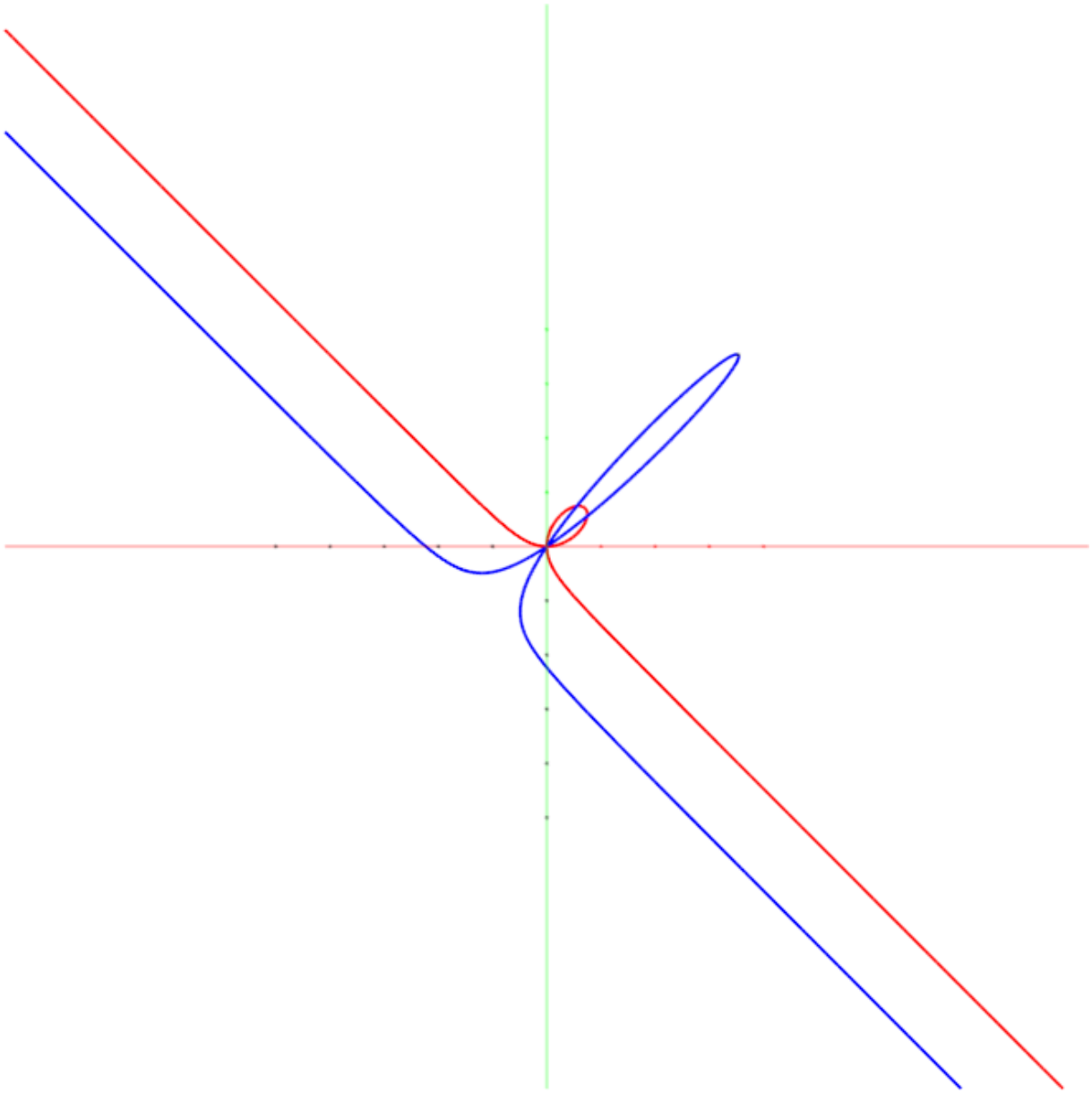

Figure 4. Directed (anisotropic) scaling of the folium of Descartes $a = 1$, dilated by $d = 5$ in the diagonal direction $\mathbf{e}_1 + \mathbf{e}_2$.

4 | IMPLEMENTATION OF TCGA

In symbolic calculations using a computer algebra software (e.g., SymPy [27] with the module $\mathcal{GA}$lgebra [1]), all implicit plane curve functions[20] $F(x, y) = 0$ can be produced by the inner product $F(x, y) = \mathbf{T}_{\mathcal{T}} \cdot \mathbf{\Omega} = 0$, where $\mathbf{T}_{\mathcal{T}}$ is the symbolic TCGA test point $\mathbf{T}_{\mathcal{T}} = \mathcal{T}\left(x\mathbf{e}_1 + y\mathbf{e}_2\right)$ with x and y as symbols, and $\mathbf{\Omega}$ is any of the TCGA IPNS 3-vector entities of Section 3.7. An implicit plane curve equation $F(x, y) = 0$ can be graphed or plotted using commonly available graphing, plotting, or scientific visualization software (e.g., MayaVi [26] using `x,y,z = mgrid[-10:10:2000j, -10:10:2000j, 0:1]` for nearly 2-D graphing around the origin; MayaVi is primarily a 3-D visualization software).

[20]Note, that for an implicit plane curve equation $F(x, y) = 0$, a point (x, y) is on the plane curve when $F(x, y) = 0$. In the neighborhood of (x, y), the function $F(x, y) = \mathbf{T}_{\mathcal{T}} \cdot \mathbf{\Omega}$ is positive on one side of the plane curve and negative on the other side of the plane curve. This can also be used to judge if a point is inside or outside a closed curve, like in Figure 2.

For example, with SymPy [27] using the $\mathcal{GA}$lgebra [1] module, the sextic implicit plane curve equation for the cranioid $\mathfrak{C}_t$ of Section 3.7.4 is generated as

$$F(x,y) = \mathbf{T}_{\mathcal{T}} \cdot \mathfrak{C}_t = 0, \tag{62}$$

where the symbolic test point $\mathbf{T}_{\mathcal{T}}$ is the TCGA point embedding $\mathcal{T}\left(\mathbf{t}_{\mathcal{E}}\right)$ of $\mathbf{t}_{\mathcal{E}^1} = x\mathbf{e}_1 + y\mathbf{e}_2$ as

$$\mathbf{T}_{\mathcal{T}} = \mathcal{T}\left(\mathbf{t}_{\mathcal{E}}\right) = C^1\left(\mathbf{t}_{\mathcal{E}^1}\right) C^2\left(\mathbf{t}_{\mathcal{E}^2}\right) C^3\left(\mathbf{t}_{\mathcal{E}^3}\right). \tag{63}$$

Figure 3 was produced by graphing $F(x,y) = 0$ using the scientific visualization software MayaVi [26], and it was annotated with mathematical text using TEXMACS [28].

Versors of high grade, operating on entities of high grade, incur high computational costs in terms of the total number of arithmetic operations involved. In general, a k-versor V_k can be factored into a product of k vectors as $V_k = \mathbf{v}_1\mathbf{v}_2 \ldots \mathbf{v}_k$, and then the versor operation can be implemented as a succession of vector reflection operations in the $\mathbf{v}_i$, which may lower the computational costs. Intelligent usage of the associativity of the geometric product can reduce the dimensions and grades of products more quickly than naïve usage, and does generally improve the efficiency of computations with the geometric product, including versor operations. In our experience it has proved optimal to compute k-CGA $\{k, 2k\}$-versor operations $A'_{\mathcal{K}} = V_{\mathcal{K}} A_{\mathcal{K}} V_{\mathcal{K}}^{-1}$ as k successions of the CGA1…k $\{1,2\}$-versor operations $A'_{\mathcal{K}} = V_{C^1}\left(V_{C^2} \ldots \left(V_{C^k} A_{\mathcal{K}} V_{C^k}^{-1}\right) \ldots V_{C^2}^{-1}\right) V_{C^1}^{-1}$ using the associativity of the geometric product (see Appendix A).

For example, the TCGA 6-versor operations (combinations of translations, dilations and rotations) were tested as successions of the three CGAi 2-versor operations for each operation, otherwise the symbolic test computations were very slow in SymPy with the $\mathcal{GA}$lgebra module (compare e.g., Fig. 2). When implementing and testing TCGA in SymPy [27] using the $\mathcal{GA}$lgebra [1] module, it is easy to create functions that return entities and versors according to parameters and to implement the successions of versor operations on the entities to transform them.

Furthermore, the anisotropic dilation operation of Section 3.8 has been successfully tested using SymPy [27] with the $\mathcal{GA}$lgebra [1] module, and it is indeed practicable for some calculations if the three 2-versors $B^{\mathbf{p}}_{\mathcal{M}^i} = T_{C^i} B_{\mathcal{M}^i} \left(T_{C^i}\right)^{\sim}$ operate on a general cubic entity $\mathbf{X}_{\mathcal{T}}$ in succession instead of directly using the 6-versor operation $B^{\mathbf{p}}_{\mathcal{T}} \mathbf{X}_{\mathcal{T}} \left(B^{\mathbf{p}}_{\mathcal{T}}\right)^{\sim}$ (see Appendix A).

5 | CONCLUSION

The Triple Conformal Geometric Algebra (TCGA or 3-CGA) $\mathcal{G}_{3(2+1),3}$ for the Euclidean plane $\mathbb{R}^2$ has IPNS 3-blade entities representing points, point pairs, lines, and circles and IPNS 3-vector entities representing general cubic plane curves and their inversions in circles (and generalizing to reflections in lines). TCGA also has IPNS 3-vector entities for representing certain types of cyclidic (or roulette) quartic, quintic, and sextic plane curves. The circle and line entities are also the operators for inversion and reflection in them, which are implemented as vector reflections. Conformal operations (as versor operations with exponential forms) for dilation, translation, and rotation of any TCGA entity can be defined in terms of inversions in circles, reflections in parallel lines, and reflections in non-parallel lines, respectively. As explained at the end of Section 3.4, for any TCGA plane curve entity representing a general cubic or certain types of quartic, quintic, or sextic curve, it is possible to form an entity representing its intersection with a line or circle. TCGA includes commutator-based differential operators applicable to any TCGA IPNS 3-blade or 3-vector entity and that provide a standard method of differentiation (or differential calculus).

As already indicated in the introduction, further extensions generalizing TCGA to k-CGAs, will allow for the definition of IPNS k-vector entities representing geometric surfaces of general degree k (and also Darboux k-cyclidic entities for surfaces of degrees $(k+1) \ldots 2k$) and their intersections with k-blade entities (k-CGA hyperplanes and hyperspheres), and algebraic differential operators of the form $D_x = kT_{x^{k-1}} T_{x^k}^{-1}$ (as products of certain extraction operators T_s) using the commutator product $\partial_x \mathbf{\Omega} = D_x \times \mathbf{\Omega}$ on any k-vector entity $\mathbf{\Omega}$ [4]. However, as the dimension $n = p + q$ of the geometric vector space $\mathbb{R}^{p,q}$ and the multiplicity k of the k-CGA increase, the dimension $k(n+2)$ of the k-CGA increases rapidly and the number of canonical algebraic basis blades $2^{k(n+2)}$ [25] increases exponentially, which may lead to impracticable computational costs unless the implementation is very efficient [11] and optimized [15][17]. Computational costs can also be reduced in the computations of versor operations by intelligent usage of the associativity of the geometric product and of the Cartan-Dieudonné theorem on orthogonal transformations to compute slow $\{k, 2k\}$-versor operations as k successions of much faster $\{1,2\}$-versor operations (see Appendix A).

ACKNOWLEDGMENTS

E. Hitzer wishes to thank God: *Soli Deo Gloria*, to thank his family and H. Suzuki for their kind support, R.B. Easter for excellent collaboration, and the ENGAGE 2017 related special issue of MMA guest editors A. Aristidou, D. Hildenbrand, and G.S. Staples. In applications of this research, please respect the Creative Peace License [22]. The authors wish to thank the anonymous reviewers for their careful reading and many excellent helpful suggestions.

References

[1] Alan Bromborsky. *Geometric Algebra Module for SymPy*. (2016). Software: https://github.com/brombo/galgebra.

[2] Fred Brackx, Richard Delanghe, and Frank Sommen. *Clifford Analysis*. Research Notes in Mathematics, Volume 76. London: Pitman Advanced Publishing Program, (1982).

[3] Leo Dorst, Daniel Fontijne, and Stephen Mann. *Geometric Algebra for Computer Science (Revised Edition): An Object-Oriented Approach to Geometry*. The Morgan Kaufmann Series in Computer Graphics. Elsevier, (2009). DOI: 10.1016/B978-0-12-374942-0.X0000-0

[4] Robert Benjamin Easter. *Differential Operators in the $\mathcal{G}_{8,2}$ Geometric Algebra, DCGA*. Original research working paper. (2015). Vixra.org preprint: 1512.0303.

[5] Robert Benjamin Easter. *$\mathcal{G}_{8,2}$ Geometric Algebra, DCGA*. Original research working paper. (2015). Vixra.org preprint: 1508.0086.

[6] Robert Benjamin Easter. *Double Conformal Space-Time Algebra*. Original research working monograph. (2016). Vixra.org preprint: 1602.0114.

[7] Robert Benjamin Easter and Eckhard Hitzer. *Conic and Cyclidic Sections in Double Conformal Geometric Algebra $\mathcal{G}_{8,2}$*. In proceedings of SSI 2016, Session SS11, 6-8 December 2016, Ohtsu, Shiga, Japan, pages 866–871. http://www.sice.or.jp/org/SSI2016/program.php#SS11. Vixra.org preprint: 1612.0221.

[8] Robert Benjamin Easter and Eckhard Hitzer. *Double Conformal Geometric Algebra for Quadrics and Darboux Cyclides*. In *Proceedings of the 33rd Computer Graphics International*, CGI 2016, pages 93–96. New York: ACM, (2016). DOI: 10.1145/2949035.2949059.

[9] Robert Benjamin Easter and Eckhard Hitzer. *Double Conformal Space-Time Algebra*. In proceedings: *AIP Conference Proceedings*, 1798(1):20066, (2017). DOI: 10.1063/1.4972658.

[10] Robert Benjamin Easter and Eckhard Hitzer. *Double Conformal Geometric Algebra*. Advances in Applied Clifford Algebras, Volume 27, Issue 3, pages 2175–2199, (2017). DOI: 10.1007/s00006-017-0784-0. Vixra.org preprint: 1705.0019.

[11] Daniel Fontijne. *Efficient Implementation of Geometric Algebra*. PhD thesis , Universiteit van Amsterdam, (2007).

[12] Gerd Fischer. *Plane Algebraic Curves*. Student Mathematical Library, Volume 15. Providence, Rhode Island, USA: American Mathematical Society, (2009).

[13] David Hestenes. *New Foundations for Classical Mechanics*. Fundamental Theories of Physics, Volume 99. Second edition. Dordrecht: Kluwer Academic Publishers, (1999).

[14] David Hestenes and Garret Sobczyk. *Clifford Algebra to Geometric Calculus, A Unified Language for Mathematics and Physics*. Fundamental Theories of Physics, Volume 5. Dordrecht: Kluwer Academic Publishers, (1984).

[15] Dietmar Hildenbrand, Justin Albert, Patrick Charrier, and Christian Steinmetz. *Geometric Algebra Computing for Heterogeneous Systems*. Advances in Applied Clifford Algebras, Volume 27, Issue 1, pages 599–620, (2017). DOI: 10.1007/s00006-016-0694-6.

[16] Dietmar Hildenbrand and Reinhard Oldenburg. *Geometric Algebra: A Foundation of Elementary Geometry with possible Applications in Computer Algebra based Dynamic Geometry Systems*. The Electronic Journal of Mathematics and Technology, Volume 9, Number 3, Special Issue (June), 19 pages, (2015). Note: Special Issue (June) contains papers from the Computer Algebra and Dynamic Geometry in Mathematics Education conference (CADGME 2014) held in September in Halle (Saale), Germany.

[17] Dietmar Hildenbrand. *Foundations of Geometric Algebra Computing*. Geometry and Computing, Volume 8. Berlin: Springer-Verlag, (2013). DOI: 10.1007/978-3-642-31794-1.

[18] Eckhard Hitzer. *Conic Sections and Meet Intersections in Geometric Algebra*. In Hongbo Li, Peter J. Olver, and Gerald Sommer (Editors), *Computer Algebra and Geometric Algebra with Applications, 6th International Workshop, IWMM 2004 Shanghai, China, May 19–21, 2004 and International Workshop, GIAE 2004 Xian, China, May 24–28, 2004, Revised Selected Papers*. Lecture Notes in Computer Science, Volume 3519, pages 350–362. Berlin, Heidelberg, New York: Springer, (2005). DOI: 10.1007/11499251_25. Arxiv.org preprint: 1306.1017.

[19] Eckhard Hitzer and Ginanjar Utama. *The GeometricAlgebra Java Package – Novel Structure Implementation of 5D Geometric Algebra $\mathbb{R}_{4,1}$ for Object Oriented Euclidean Geometry, Space-Time Physics and Object Oriented Computer Algebra*. Mem. Fac. Eng. Univ. Fukui 53(1), pp. 47–59 (2005). Vixra.org preprint: 1306.0120.

[20] Eckhard Hitzer, Kanta Tachibana, Sven Buchholz, and Isseki Yu. *Carrier Method for the General Evaluation and Control of Pose, Molecular Conformation, Tracking, and the Like*. Advances in Applied Clifford Algebras, Volume 19, Issue 2, pages 339–364, (2009). DOI: 10.1007/s00006-009-0160-9.

[21] Eckhard Hitzer. *Introduction to Clifford's Geometric Algebra*. SICE Journal of Control, Measurement, and System Integration, Volume 51, Number 4, pages 338–350, (April 2012). Arxiv.org preprint: 1306.1660.

[22] Eckhard Hitzer. *Creative Peace License*. (2011). https://gaupdate.wordpress.com/2011/12/14/the-creative-peace-license-14-dec-2011/ [Online; accessed 13 Feb. 2017].

[23] Hongbo Li, David Hestenes, and Alyn Rockwood. *Generalized Homogeneous Coordinates for Computational Geometry*. In Gerald Sommer (Editor), *Geometric Computing with Clifford Algebras. Theoretical Foundations and Applications in Computer Vision and Robotics*, chapter 2, pages 27–59. Berlin: Springer, (2001). DOI: 10.1007/978-3-662-04621-0.

[24] J. Dennis Lawrence. *A Catalog of Special Plane Curves*. New York: Dover Publications, (1972).

[25] Christian Perwass. *Geometric Algebra with Applications in Engineering*. Geometry and Computing, Volume 4. Berlin: Springer, (2009). DOI: 10.1007/978-3-540-89068-3.

[26] Prabhu Ramachandran and Gaël Varoquaux. *Mayavi: 3D Visualization of Scientific Data*. Computing in Science & Engineering, Volume 13, Issue 2, pages 40–51, (2011). DOI: 10.1109/MCSE.2011.35.

[27] SymPy Development Team. *SymPy: Python library for symbolic mathematics*. (2016). Software: http://sympy.org.

[28] Joris van der Hoeven, Andrey Grozin, Massimiliano Gubinelli, Grégoire Lecerf, François Poulain, and Denis Raux. *GNU TEXmacs: a scientific editing platform*. ACM SIGSAM Communications in Computer Algebra, Volume 47, Issue 1/2, pages 59–61, (March/June 2013). DOI: 10.1145/2503697.2503708.

APPENDIX A: ON EFFICIENT USAGE OF ASSOCIATIVITY IN VERSOR OPERATION COMPUTATIONS

An *intelligent (efficient) usage* of the associativity of the geometric product is to associate groups of factors in a chain of geometric products into parentheses, changing the order of multiplications, to reduce or minimize the total number of algebra operations or computational costs (in runtime) that are required as compared to the *naïve (inefficient) usage* of the associativity of the geometric product, which is the default (usually left to right) order of multiplication of the factors. Different choices of associative groupings in parentheses to order the products may be more or less efficient (or expensive) than each other according to computational costs

(usually measured by runtime). To determine the most intelligent (efficient) usage requires gathering intelligence in the form of estimates of computational costs for alternative usages and then intelligently choosing the usage that minimizes computational costs.

As an example of a naïve usage of the associativity of the geometric product, consider the versor "sandwich" operation $\mathbf{\Omega}' = \mathbf{C}_{\mathcal{T}}\mathbf{\Omega}\mathbf{C}_{\mathcal{T}}^{\sim} = \mathbf{C}_{\mathcal{C}^1}\mathbf{C}_{\mathcal{C}^2}\mathbf{C}_{\mathcal{C}^3}\mathbf{\Omega}\mathbf{C}_{\mathcal{C}^3}\mathbf{C}_{\mathcal{C}^2}\mathbf{C}_{\mathcal{C}^1}$ for the inversion of a TCGA IPNS 3-vector entity $\mathbf{\Omega}$ in a TCGA IPNS 3-blade *standard circle* (3-versor *inversor*) $\mathbf{C}_{\mathcal{T}} = \mathbf{C}_{\mathcal{C}^1}\mathbf{C}_{\mathcal{C}^2}\mathbf{C}_{\mathcal{C}^3}$. The TCGA circle $\mathbf{C}_{\mathcal{T}}$ is factored into the product of the three corresponding CGA*i* circles $\mathbf{C}_{\mathcal{C}^i}$. Each CGA*i* IPNS 1-blade *circle* (1-versor *inversor*) $\mathbf{C}_{\mathcal{C}^i}$ is a vector with up to four component terms. Without any parentheses to perform the three vector reflections in succession, the six geometric products in $\mathbf{\Omega}'$ are evaluated in the default (left to right) order. Assuming that *like terms* are added during each of the six multiplications, this naïve usage requires up to $4^2+4^3+4^3\times 64+4\times\sum_{i=0,2,4,6}\binom{12}{i}+4\times\sum_{i=1,3,5,7}\binom{12}{i}+4\times\sum_{i=0,2,4,6,8}\binom{12}{i} = 16+64+4096+4\times 1486+4\times 1816+4\times 1981 = 25308$ basis blade multiplications to compute $\mathbf{\Omega}'$.

A more intelligent usage of the associativity of the geometric product is $\mathbf{\Omega}' = \mathbf{C}_{\mathcal{C}^1}\left(\mathbf{C}_{\mathcal{C}^2}\left(\mathbf{C}_{\mathcal{C}^3}\mathbf{\Omega}\mathbf{C}_{\mathcal{C}^3}\right)\mathbf{C}_{\mathcal{C}^2}\right)\mathbf{C}_{\mathcal{C}^1}$, with parentheses to associate each successive vector reflection as three nested vector reflections. This requires up to $3\times 64\times(4+4^2) = 3840$ basis blade multiplications if each successive vector reflection in parentheses transforms up to 64 terms in $\mathbf{\Omega}$ into another 64 transformed terms (this depends on adding like terms during each successive vector reflection).

Another choice (usage) of associativity is $\mathbf{\Omega}' = \left(\mathbf{C}_{\mathcal{C}^1}\mathbf{C}_{\mathcal{C}^2}\mathbf{C}_{\mathcal{C}^3}\right)\mathbf{\Omega}\left(\mathbf{C}_{\mathcal{C}^3}\mathbf{C}_{\mathcal{C}^2}\mathbf{C}_{\mathcal{C}^1}\right) = \mathbf{C}_{\mathcal{T}}\mathbf{\Omega}\mathbf{C}_{\mathcal{T}}^{\sim}$. With this choice, $\mathbf{\Omega}'$ requires up to $2\times 4^3+4^3\times 64+4^3\times\sum_{i=0,2,4,6}\binom{12}{i} = 128+4096+95104 = 99328$ basis blade multiplications, which is more naïve (less efficient or intelligent) than the default (left to right) associativity. After the multiplications, like terms could be added, resulting in up to 64 transformed 3-blade terms. It is possible that this choice would be the first choice used by a novice, but it is, perhaps surprisingly, the most naïve (inefficient). There are still other possible choices (usages) of the associativity in computing $\mathbf{\Omega}'$, which may each have different computational costs.

For the example choices discussed above, the successive (nested) vector reflections appear to be most efficient, requiring the least basis blade multiplications. In a parallel computing environment, a nested expression may not be the most efficient or intelligent choice for minimizing runtime. In applications that use precomputed results, the final results are the same for all choices of associativity after all like terms are added; however, the computational costs to precompute the results may depend on the choice of associativity during the precomputing, leading to faster or slower precomputation.

AUTHOR BIOGRAPHY

Robert Benjamin Easter. First author. R.B. Easter is an American, born April 4, 1972 in Sarasota, Florida U.S.A., that has been living in Bangkok, Thailand while performing mathematical research and authoring mathematical papers. DCGA (2-CGA), TCGA (3-CGA), and generalizing to k-CGA were conceived by R.B. Easter as extensions of CGA (1-CGA) with k-vector geometric entities that represent general degree k polynomial implicit hypersurfaces and their inversions as special hypersurfaces of up to degree $2k$. R.B. Easter is the author of the original papers and manuscripts on DCGA, TCGA, and k-CGA. The works of R.B. Easter can be found at http://orcid.org/0000-0002-8725-1835 and at http://vixra.org/author/robert_b_easter. R.B. Easter prepared this revised TCGA preprint paper with corrections and improvements to the published version.

Eckhard Hitzer. Second author. E. Hitzer jointly prepared the revisions for publication with R.B. Easter, including corresponding with the publishing editors and responding to the peer reviewers. E. Hitzer also presented the TCGA paper (by preparing and presenting a 38-slide PDF presentation based on the original pre-submission TCGA manuscript and other referenced works) at the Empowering Novel Geometric Algebra in Graphics and Engineering (ENGAGE) Workshop (Session: ENGAGE III, June 27 14:00–15:30) at the Computer Graphics International 2017 (CGI2017) conference (June 27-30, 2017 / Yokohama, Japan).

How to cite this article: Robert Benjamin Easter and Eckhard Hitzer, (2018), Triple Conformal Geometric Algebra for Cubic Plane Curves, *Mathematical Methods in the Applied Sciences*, *2018;41(11):4088–4105*.